Rapamycin Regulates Autophagy and Cell Adhesion in Induced Pluripotent Stem Cells

Stem Cell Research & Therapy

Rapamycin Regulates Autophagy and Cell Adhesion in Induced Pluripotent Stem Cells

--Manuscript Draft--

Manuscript Number:	SCRT-D-16-00129R1
Full Title:	Rapamycin Regulates Autophagy and Cell Adhesion in Induced Pluripotent Stem Cells
Article Type:	Research
Funding Information:	Science Foundation Ireland (09/SRC B1794) — Prof Sanbing Shen Science Foundation Ireland (09/SRC/B1794s1) — Prof Sanbing Shen SFI Investigator Programme (13/IA/1787) — Prof Sanbing Shen SFI TIDA program (14/TIDA/2258) — Prof Sanbing Shen NUI Galway (RSU002) — Prof Sanbing Shen
Abstract:	Background: Cellular reprogramming is a stressful process, which requires cells to engulf somatic features, produce and maintain stemness machineries. Autophagy is a process to degrade unwanted proteins and required for the derivation of induced pluripotent stem cells (iPSCs). However, the role of autophagy during iPSC maintenance remains undefined. Methods: Human iPSCs were investigated by microscopy, immunofluorescence and immunoblotting to detect autophagy machinery. Cells were treated with Rapamycin to activate autophagy and Bafilomycin to block autophagy during iPSC maintenance. High concentrations of Rapamycin treatment, unexpectedly, resulted in spontaneous formation of round floating spheres of uniform size, which were analyzed for differentiation into three germ layers. Mass spectrometry was deployed to reveal altered protein expression and pathways associated with Rapamycin treatment. Results: We demonstrate that human iPSCs express high basal levels of autophagy, including key components of APMKα, ULK1/2, BECLIN-1, ATG13, ATG101, ATG12, ATG3, ATG5 and LC3B. Block of autophagy by Bafilomycin induces iPSC death and Rapamycin attenuates the Bafilomycin effect. Rapamycin treatment up-regulates autophagy in iPSCs in a dose/time-dependent manner. High concentration of Rapamycin reduces NANOG expression and induces spontaneous formation of round and uniformly sized embryoid bodies (EBs) with accelerated differentiation into three germ layers. Mass spectrometry analysis identifies actin cytoskeleton and adherens junctions as the major targets of Rapamycin in mediating iPSC detachment and differentiation. Conclusions: High levels of basal autophagy activity are present during iPSC derivation and maintenance. Rapamycin alters expression of actin cytoskeleton and adherens junctions, induces uniform EB formation and accelerates differentiation. IPSCs are sensitive to enzyme dissociation and require lengthy differentiation time. The shape and size of EBs also play a role in the heterogeneity of end cell products. Therefore, this research highlights the potential of Rapamycin in producing uniform EBs and in shortening iPSC differentiation duration.
Corresponding Author:	Sanbing Shen, BSc, MSc, PhD NUI Galway Galway, IRELAND
Corresponding Author Secondary Information:	
Corresponding Author's Institution:	NUI Galway
Corresponding Author's Secondary Institution:	
First Author:	Areechun Sotthibundhu
First Author Secondary Information:	

Order of Authors:	Areechun Sotthibundhu
	Katya McDonagh
	Alexander von Kriegsheim
	Amaya Garcia-Munoz
	Agnieszka Klawiter
	Kerry Thompson
	Kapil Dev Chauhan
	Janusz Krawczyk
	Veronica McInerney
	Peter Dockery
	Michael J Devine
	Tilo Kunath
	Frank Barry
	Timothy O'Brien
	Sanbing Shen, BSc, MSc, PhD
Order of Authors Secondary Information:	
Response to Reviewers:	Point-to-point Response Reviewer reports: Reviewer #1: This is an interesting investigation into the role of autophagy in iPSC function, and builds on the growing body of work demonstrating the key role of autophagy in stem cell biology. The authors show a higher level of autophagy at basal conditions in iPSCs over their parental fibroblasts, which can be modulated in a dose-dependent manner with rapamycin to affect the iPSC maintenance in culture and EB formation/differentiation over time. RESPONSE: We thank Reviewer #1 for careful reading and recognition of the key points of the manuscript. General comments: - The English in the manuscript would benefit from revision. Several areas are in need of editing for clarity, and there are a high number of errors/typos throughout the manuscript. RESPONSE: We apology for the errors/typos in the previous versions. The Manuscript has now been gone through several edits and hope the revised version is substantially improved. - Avoid including discussion of the results in the Results section (e.g. discussion of the results in Fig 2) RESPONSE: The introductory contents in section 2 and 3 of the Results on pages 11-12 are now shortened. Specific comments: I appreciated the demonstration of high LC3II levels across four separate donors in the iPSC population. I would perhaps suggest including LC3I levels at least in the blot in 2E to show whether there is an upregulation of autophagosome accumulation/cycling, or a block in autophagosome degradation that causes the shift. Some recent studies have shown stem cell populations to have very low degrees of autophagosome cycling at a basal state. RESPONSE: We acknowledge that The Reviewer #1 brought up an interesting point of the autophagosome cycling. This manuscript has addressed several points: high level of the autophagy is crucial for iPSC physiology and maintenance, and induced autophagy by Rapamycin is associated with cell detachment and EB formation

together with accelerated differentiation.

In the revised version, we have new data to further strengthen the importance of autophagy in iPSCs, that block of autophagy by Bafilomycin induces cell death and Rapamycin rescues Bafilomycin-induced cell death (See Lines 303-320 and new Figure 5). We also provide new mechanistic data for accelerated differentiation that Rapamycin downregulates NANOG expression in a concentration-dependent manner (See Figure 8L-M, and lines 355-362, 767-771).

We kept the original Figure 2 which was done on 10% SDS-PAGE. The data showed that (1) Rapamycin can induce autophagy in both iPSCs and fibroblasts, and (2) both the basal and induced autophagy activities are higher in iPSCs. We have now provided a Supplemental Figure 1 to show that two bands of LC3B-I (16kD) and LC3B-II (14kD) can be better resolved on 15% SDS-PAGE. The new data brought up an interesting point that Rapamycin increased LC3B-I rather than LC3B-II expression in fibroblasts (Supplemental Figure 1), and this is different from iPSCs (see Figure 4), and will require further investigation and is therefore provided as a Supplemental Figure, to avoid diversion of the focus. See Line 299-301.

: The overall goal of this figure seems to be to show high levels of autophagy signaling molecules across several iPSC lines. Demonstrating the activation of autophagy signaling is important, but it is difficult to discern levels of activation with no outside standard for comparison in this figure (all relative abundance measurements are made using each individual sample as its own control). I would suggest including a lane or two of parental fibroblasts or other control cells to serve as a comparison as you did in Figure 2.
RESPONSE: We appreciate Reviewer #1's comments, carried out new experiments and included new data in the revised Figure 3H. Consistent with other data shown in the manuscript, both ATG5 and ATG12 are more abundant in iPSCs than that in parental fibroblasts. See revised Figure 3H and lines 280-283

It is also unclear why samples a-e are assayed for ATGs but not f-l. Error bars are missing from Fig 3G.
RESPONSE: This reflected the history of iPSC availability in the group. We first carried out series of WB on 5 lines (a-e, see Figure 3A-B) with three repeated blots. When additional 7 iPSC lines "f-l" became available, we further strengthen the point by using iPSC line "b" as a reference in the new Western blots. These lines were done only once (Figure 3C and G), but the data were consistent with 5 lines in A-B, Figure 3A,B,D-F.

Fig 5/6: Results investigating the iPSC maintenance focus solely on the rapamycin dosing. Inhibition of autophagy with bafilomycin or another treatment is not discussed in this study much. If rapamycin benefits iPSC maintenance and differentiation, how does inhibiting the pathway affect things? Some studies on stem cell autophagy have shown conflicting roles of rapamycin and bafilomycin treatments on the function of autophagy.
RESPONSE: We appreciate Reviewer #1 for expert opinion. We carried out additional experiments with bafilomycin A1 as suggested. The new data showed that bafilomycin induced dose-dependent cell death whereas Rapamycin can rescue Bafilomycin-induced cell death (See lines 303-320 and new Figure 5). This further highlights the importance of autophagy in iPSCs.

Fig 8: Given that the authors showed an optimal Rapamycin response of 200 nM in Fig 4 and used this dose for subsequent EB experiments in Figs 5-7, it is unclear why 50 and 100 uM doses are used in this experiment, which are substantially higher doses.
RESPONSE: Apology for the typos. we used 50 and 100 nM (not uM) in proteomics assays.

Discussion: The discussion focuses largely on results from Fig 8, which seems minor compared to the rest of the manuscript that focuses on the specific autophagic character and response in the iPSCs examined here. Some points for consideration in the discussion:
- Fig 2 shows two donors having different basal levels of autophagy (a/b vs c/d). How will donor variability affect these results, or even different iPSC parent sources?

- Do the authors feel that a particular set of culture conditions here are suitable for recommended use in standard iPSC culture? How should rapamycin be used most efficiently to benefit iPSC maintenance, differentiation, etc?
- EBs assayed in Fig 7 show a high level of LC3-I compared to the control EBs. Speculation as to why? How does the basal level of cytosolic LC3/autophagosome cycling and accumulation affect this function of iPSCs?
RESPONSE: many thanks to Reviewer 1 for constructive advice. We revised Discussion accordingly

Reviewer #2: The manuscript by Sotthibundhu A and colleagues describes that inhibition of mTOR signaling pathway by rapamycin could regulates autophagy and cell adhesion in induced pluripotent stem cells. The group highlights that the potential of rapamycin in producing uniform embryoid bodies and in accelerating iPSCs differentiation.
Overall, the manuscript is interesting and will contribute to the current understanding of iPSCs biology. It is of particular interest and may encourage further studies into this area about the role of autophagy during iPSC maintenance. However, the work as developed is largely confirmatory of previous findings and while there is some new information, such is limited. For example, it is well established that autophagy could be regulated by mTOR pathway, and regulation of embryoid body formation by mTOR pathway was also reported (Oncogene 2010).
RESPONSE: We thank Reviewer #2 for bringing up this literature, which is different from our data with different cell types. The paper is cited as Ref 40 and discussed in lines 413-416 .

My critiques:
1. In figure 1A, images showing autophagic vacuoles of fibroblasts without reprogramming should also be shown. In panel H-K, its better to show the colocalization of autophagy, lysosome, Golgi and ER markers in the same cell
RESPONSE: Thank Reviewer #2 for constructive comments. We now added a bright field image of fibroblasts in new Figure 1F. We carried out double staining as suggested and included in new Figure 1C,D,G,H.

2. In figure 2F&G, it seems that LC3BII in iPSCs showed similar increase (about 2.5 folds) that fibroblasts, no matter the cells were treated with rapamycin or not. How it can be concluded that autophagy is rapamycin-inducible?
RESPONSE: Figure 2F showed the difference of basal LC3B between fibroblasts and iPSCs. Figure 2G showed relative LC3B activity between fibroblasts and iPSCs after Rapamycin treatment. Rapamycin can induce LC3B in both fibroblasts and iPSCs. See lines 255-265.

3. In figure 3, the results of fibroblasts as negative control should also be shown.
RESPONSE: Thank Reviewer #2 for the suggestion. I have now included new data on Figure 3H, showing ATG5 and ATG12 are higher in iPSCs than in fibroblasts.

4. The figure 5F and figure 6E are the same image, please change either of them
RESPONSE: Many thanks to Reviewer #2 for careful reading. We have now removed the duplicated image, see revised Figure 7.

5. What's the difference among figure 7J, K and L?
RESPONSE: Many thanks. We have now removed K and L, and added new mechanistic data of reduced NANOG expression by Rapamycin treatment see revised Figure 8.

Rapamycin Regulates Autophagy and Cell Adhesion in Induced Pluripotent Stem Cells

Areechun Sotthibundhu[1,8], Katya McDonagh[1], Alexander von Kriegsheim[2], Amaya Garcia-Munoz[2], Agnieszka Klawiter[1], Kerry Thompson[3], Kapil Dev Chauhan[1], Janusz Krawczyk[4] Veronica McInerney[5], Peter Dockery[3], Michael J Devine[6,7], Tilo Kunath[6], Frank Barry[1], Timothy O'Brien[1], Sanbing Shen[1*]

[1] Regenerative Medicine Institute, School of Medicine, National University of Ireland (NUI) Galway, Galway, Ireland.

[2] Systems Biology Ireland, Conway Institute, University College Dublin, Dublin 4, Ireland

[3] Centre for Microscopy and Imaging, Anatomy, School of Medicine, NUI Galway, Ireland

[4] Department of Haematology, Galway University Hospital

[5] HRB Clinical Research Facility, NUI Galway, University Road, Galway Ireland

[6] MRC center for Regenerative Medicine, The University of Edinburgh, UK

[7] Department of Molecular Neuroscience, Institute of Neurology, University College London, London WC1N 3BG, UK

[8] Chulabhorn International College of Medicine, Thammasat University, Patumthani, 12120, Thailand

Email addresses: areechuns@gmail.com; katya.mcdonagh@gmail.com; kriegsheim@gmail.com; Amaya.GarciaMunoz@ucd.ie; a.klawiter.08@aberdeen.ac.uk; Kerry.Thompson@nuigalway.ie; kapil.dev@nuigalway.ie; Janusz.Krawczyk@hse.ie; Veronica.Mcinerney@nuigalway.ie; Peter.Dockery@nuigalway.ie; michael.devine.09@ucl.ac.uk; tilo.kunath@ed.ac.uk; frank.barry@nuigalway.ie; timothy.obrien@nuigalway.ie; sanbing.shen@nuigalway.ie.

* Corresponding author: Sanbing Shen, Regenerative Medicine Institute, School of Medicine, NUI Galway, Galway, Ireland, Tel:+353 91 494261, email: sanbing.shen@nuigalway.ie

Abstract

Background: Cellular reprogramming is a stressful process, which requires cells to engulf somatic features, produce and maintain stemness machineries. Autophagy is a process to degrade unwanted proteins and required for the derivation of induced pluripotent stem cells (iPSCs). However, the role of autophagy during iPSC maintenance remains undefined.

Methods: Human iPSCs were investigated by microscopy, immunofluorescence and immunoblotting to detect autophagy machinery. Cells were treated with Rapamycin to activate autophagy and Bafilomycin to block autophagy during iPSC maintenance. High concentrations of Rapamycin treatment, unexpectedly, resulted in spontaneous formation of round floating spheres of uniform size, which were analyzed for differentiation into three germ layers. Mass spectrometry was deployed to reveal altered protein expression and pathways associated with Rapamycin treatment.

Results: We demonstrate that human iPSCs express high basal levels of autophagy, including key components of APMKα, ULK1/2, BECLIN-1, ATG13, ATG101, ATG12, ATG3, ATG5 and LC3B. Block of autophagy by Bafilomycin induces iPSC death and Rapamycin attenuates the Bafilomycin effect. Rapamycin treatment up-regulates autophagy in iPSCs in a dose/time-dependent manner. High concentration of Rapamycin reduces NANOG expression and induces spontaneous formation of round and uniformly sized embryoid bodies (EBs) with accelerated differentiation into three germ layers. Mass spectrometry analysis identifies actin cytoskeleton and adherens junctions as the major targets of Rapamycin in mediating iPSC detachment and differentiation.

Conclusions: High levels of basal autophagy activity are present during iPSC derivation and maintenance. Rapamycin alters expression of actin cytoskeleton and adherens junctions, induces uniform EB formation and accelerates differentiation. IPSCs are sensitive to enzyme

dissociation and require lengthy differentiation time. The shape and size of EBs also play a role in the heterogeneity of end cell products. Therefore, this research highlights the potential of Rapamycin in producing uniform EBs and in shortening iPSC differentiation duration.

Key words

Actin cytoskeleton, Adherens junctions, Autophagy, Differentiation, Embryoid Body, Induced Pluripotent Stem Cells, Rapamycin

Background

The induced pluripotent stem cell (iPSC) technology enables conversion of patient's somatic cells into embryonic stem (ES)-like cells [1], which can be differentiated into the major cell types in the body, raising the expectation of personalized medicine to treat patients with own somatic tissue-derived cells. This also offers an opportunity to generate human cell models of diseases for therapeutic development, which has not kept pace with pharmaceutical investment in recent decades. A major impediment to drug discovery is attributable to the lack of suitable disease models of human origin, as species differences may totally affect drug efficacy [2]. Some disease pathologies are shown to be re-capitulated in the culture dish. For example, many patient-specific iPSCs have been generated to investigate disease progression *in vitro* and disease-related phenotypes are partially preserved in iPSC-derived cells [3-6]. Recent successes in the growth of "mini-organ", i.e., 3D retina [7-8] and cerebral organoids [9], may provide 3-D human disease models. However, there are challenges in phenotyping iPSCs prior to the development of screening assays, which include lengthy differentiation durations and heterogeneity of the end cell products.

The differentiation, survival and self-renewal of human stem cells can be regulated by a 3D microenvironment including shape and size [7-9,10]. Human iPSCs are hyper-sensitive to cell dissociation reagents, and seconds of exposure to Trypsin/EDTA may lead to failure of iPSC adhesion or survival. Consequently, many laboratories adopt "cut-and-paste" method to mechanically passage iPSCs, which results in EBs of uncontrollable sizes with irregular shapes, which may potentially contribute to the heterogeneity. The differentiation of mature cell types from human iPSCs is also time-consuming. For example, 3~5 months are required to generate functional neurons, astrocytes or oligodendrocytes [11-13]. Therefore, accelerated differentiation remains to be optimized.

Efforts have been made to improve the reprogramming efficiency, and autophagy, a process to degrade unwanted proteins, is found as one of the regulators during cellular reprogramming [14-15]. Autophagy is conserved from yeast to mammals, and is generally induced by intra- and extra-cellular stress. Upon induction, the preautophagosomal structure is formed and elongated to form a phagophore, which engulfs cytoplasmic components, leading to the formation of autophagosomes with double membranes. The genes involved in the autophagy are termed Autophagy-Related Genes (*ATG*s), and >12 *ATGs* have been identified. They regulate autophagosome formation through two evolutionarily conserved ubiquitin-like conjugation systems, the ATG12-ATG5 and the ATG8 (LC3)-PE (phosphatidylethanolamine) systems [16]. The LC3B-I (microtubule-associated proteins 1A/1B light chain 3-I) is conjugated with PE to become LC3B-II, which associates with both the outer and inner membranes of the autophagosome. After fusion with the lysosome, the autolysosome is degraded [17]. In mice, Atg3, Atg5 and Atg7 are essential for reprogramming of mouse embryonic fibroblasts [14-15]. Cells lacking Atg3, Atg5 or Atg7 abrogated iPSC colony formation [15].

The autophagy pathway can be activated by AMPK signaling, but is normally inhibited by the mammalian target of the Rapamycin (mTOR) pathway. The presence of hyperactivated mTOR

activity in *Tsc2*$^{-/-}$ somatic cells completely blocked reprogramming [14]. Consistent with this, Rapamycin - an inhibitor of the mTOR pathway at 0.3-1 nM could increase reprogramming efficiency by 2~3 folds [18]. In addition, 0.1 nM of PP242, a selective inhibitor of mTORC1/mTORC2 binding at the ATP domain, also increased reprogramming efficiency by 5-folds [18]. Other compounds associated with autophagy such as PQ401- an IGF1 receptor inhibitor and LY294002 - an inhibitor of PI3K also increased reprogramming by 4-folds [18]. Mechanistically, mTOR is regulated by SOX2, one of the four reprogramming factors. SOX2 can physically bind to the mTOR promoter and repress mTOR expression thereby activate autophagy [15]. Therefore, an appropriate level of autophagy is required for cell reprogramming. However, roles of autophagy in iPSC maintenance and differentiation remain elusive.

In this study, we showed the presence of high levels of basal autophagy activity during iPSC reprogramming and maintenance. Rapamycin alters expression of adherens junctions and actin cytoskeleton, induces iPSC detachment, and results in uniform EB formation. Rapamycin treatment also accelerates differentiation of human iPSCs into three germ-layers.

Methods

iPSC derivation

On day 0, human fibroblasts were seeded at a density of $2.0x10^4$ cells/well on a 6-well dish. Next day, cells were transduced with a polycistronic (OKSM) lentivirus containing four reprogramming factors (SCR544- Human STEMCCA constitutive lentivirus reprogramming kit, Millipore, SCR544) in 700 µl of fibroblast medium, supplemented with 4µg/ ml polybrene (Millipore, TR-1003). On day 2, cells were repeatedly transduced with lentivirus. The medium was then replaced daily with complete fibroblast medium supplemented with 0.25 mM sodium

butyrate (NaB, Sigma, 156-54-7) for 4 days. On day 6, 6-well dishes were pre-seeded with γ-irradiated MEF (VH Bio Limited, 07GSC6001G) at a density of $1.5x10^5$ cells/well. On day 7, transduced cells were trypsinized with 0.25% Trypsin/EDTA, and replated onto pre-seeded MEF dishes at a density of $3.0x10^4$ cells/well, and cultured in KO iPSC medium supplemented with 10ng/ml bFGF (Peprotech, 100-18B) plus 0.25 mM NaB. The medium was changed every other day. The addition of NaB was discontinued after day 20.

Individual iPSC colonies began to emerge after day 14 and were picked up on day 28, mechanically dissociated into smaller pieces by pipetting and plated into γ-MEF coated 12-well plates. Selected clones were characterized using alkaline phosphatase activity, RT-PCR and immunoblotting to detect endogenous expression of OCT4, SOX2 and NANOG, and immunocytochemistry to detect surface markers of SSEA4, TRA 1-60 and TRA 1-81 in addition to the transcription factors (StemLight™ pluripotency antibody kit, cell signaling, 9656).

Cell culture

Human iPSC lines were maintained on a feeder-free culture system. The 6-well plates were pre-coated with Geltrex, LDEV-free hESC qualified reduced growth factor basement membrane matrix (Invitrogen, A1413302). Geltrex was thawed overnight at 4˚C and diluted 1:100 in KO-DMEM medium (Invitrogen, 10829018). Each well was coated with 1.5 ml Geltrex, incubated for one hour at 37˚C, and was then replaced with the mTeSR1 medium (StemCell Technologies, 05850) with 10 ng/ml bFGF at 37°C and 5% CO_2. iPSCs were cut and paste into Geltrex-coated wells. The medium was renewed daily and passaged every 6 days. Then, chemicals such as Rapamycin were added to respective experiments.

For induction of autophagy signaling, iPSC colonies were cultured in mTeSR1 medium supplemented with 0-300 nM Rapamycin (Sigma, R8781) for 1-9 days. For autophagic flux assay, human iPSCs were treated with 200 nM Rapamycin in the absence or presence of 50

nM Bafilomycin A1 for 24 hrs (Sigma, B1793) as specified. Cells were collected and protein was subsequently analyzed by immunoblotting.

EB formation by cut-and-paste method

The cut-and-paste method was deployed to make conventional EBs as iPSCs. Spontaneously differentiated cells were removed under a stereomicroscope inside the culture safety cabinet, and fresh medium was added to the remaining iPSC colonies, which were cut into small pieces with 10ul pipette tip. The iPSC sections were then scraped off the dish and transferred to a T25 flask in 15ml EB medium (KO DMEM, KO serum, 1X L-glut and 1X NNEA plus 50ul beta-mercaptoethanol). The medium was changed every other day, and the EBs were cultured for 7-10 days before plating out for spontaneous differentiation assays.

Antibodies and reagents

The reagents for TEM include Sodium cacodylate (C0250, Sigma), low viscosity resin kit (AGR1078A, Agar Scientific) and 2 % osmium tetroxide (AGR1016, Agar Scientific), 25 % Glutaraldehyde Solution (23114.02**,** AMSBIO), and thermanox plastic coverslips (NUNC). For immunocytochemistry, following antibodies were used: anti-LAMP1 (25630), anti-Syntaxin-6 (12370), and anti-NESTIN (105389) from Abcam; SelectFX® Alexa Fluor® 488 Endoplasmic Reticulum labeling kit (S34200) from Life Technologies; anti-LC3B from autophagy antibody sampler kit (4445), Alexa Fluor® 488 Goat Anti-Rabbit IgG fluorescent dye (4412), and Alexa Fluor® 555 Goat Anti-Mouse IgG fluorescent dye (4409) from Cell Signaling Technology. For immunoblot experiments, reagents included anti-α-fetoprotein (A8452), anti-α-smooth muscle actin (A2547), anti-ATG13 (SAB3500502) and ATG101 (SAB3500503) from Sigma; anti-βIII tubulin (G7121) from Promega Corporation; anti-ULK2 (56736) from Abcam; anti-LC3B, anti-BECLIN-1, anti-ATG5 from Cell Signalling Technology (D1G9; #8540P, 1:1000) anti-ATG12, and anti-ATG3 from autophagy antibody

sampler kit (4445), anti-p-ULK1(Ser317, 6887), anti p-p70 S6K (Thr389, 9205), anti-β-Actin (4967), HRP-conjugated anti-mouse IgG antibody (7076) and HRP-conjugated anti-rabbit-IgG antibody (7074) from Cell Signaling Technology. MitoGreen (a Green-fluorescent mitochondrial dye) was purchased from Promokine (PK-CA707-70054).

Transmission electron microscopy (TEM)

iPSCs were cultured on Thermanox coverslips in 6-well plates coated with Geltrex, rinsed with prewarmed (37^{o}C) 0.1M cacodylate buffer, fixed with 2% Glutaraldehyde and 2% Paraformaldehyde in 0.1M cacodylate buffer for 3 hours at room temperature, rinsed again with cacodylate buffer and post-fixed with 1% osmium tetroxide in cacodylate for 1hr at room temperature. Samples were then rinsed with cacodylate buffer, dehydrated through a series of graded ethanol, embedded in low viscosity resin according to the standard protocol, and polymerized at 60^{o}C for 48hrs. Ultra-thin sections were obtained using a diamond knife, on a Leica Reichert Jung ultra-microtome, and stained with the contrasting agents, uranyl acetate and lead citrate, in a Leica EM AC20 stainer. Sections were examined with a Hitachi H7000 transmission electron microscope fitted with a 1K Hamamatsu Digital Camera and images were captured using AMTV542 Image Capture Engine software.

Immunocytochemistry

To investigate the effect of Rapamycin, iPSC colonies or the embryoid body-like spheres were transferred to µ-Slide 8-well glass bottom (ibidi GmBH, 80826) coated with Geltrex. Cells were fixed with 4% paraformaldehyde for 10 min at room temperature and washed with PBS 3 times before permeabilization using 0.5% Triton X-100 for 10 min. Non-specific binding was blocked with 5% normal goat serum in PBS containing 0.5% Trion X for 1hr prior to incubation with primary antibodies overnight at 4˚C. The wells were washed three times with PBS and incubated with secondary antibodies for 1hr at room temperature. The nuclei were visualized by Hoechst counterstaining for 10 min. After washing with PBS, the immunofluoresence was visualized with

the Andor Revolution spinning disk confocal microscope, using Andor IQ2 software. The samples were imaged using a combination of λ405nm, λ488nm and λ564nm lasers.

Immunoblotting

Following experimental treatments, cell pellets were resuspended in NP40 cell lysis buffer (Invitrogen, FNN0021) supplemented with protease inhibitor cocktail (Sigma, P2714). Lysate was then centrifuged at 13,000 rpm for 10 min at 4°C, and the supernatant was collected and used for immunoblotting. Protein concentration was determined and the samples were denatured in sample buffer (62.5 mM Tris–HCl pH 6.8, 2% SDS, 10% glycerol, 2% mercaptoethanol and 0.01% bromophenol blue) at 95°C for 5 min. Proteins were resolved on 10-15% SDS–PAGE gels and then electrophoretically transferred to a polyvinylidene difluoride (PVDF) membrane (Bio-Rad, 162-0177). The transfer efficiency was checked by Ponceau-S red staining (Sigma, P7170). The membranes were washed with Tris-buffered saline containing 0.1% Tween-20 (TBST) for 5 min, incubated in blocking buffer for 1hr at room temperature and incubated overnight at 4°C with primary antibodies. They were then washed three times for 5 min each with TBST, incubated with secondary antibodies for 1hr at room temperature and washed in TBST. Finally, the membranes were visualized by enhanced chemiluminescence using ECL™ Prime (Amersham Biosciences, GZ28980926). The immunoblot band densities were normalized with its unphosphorylated protein or Actin or GAPDH, and quantified using a densitometer in the Scion image analysis program (National Institutes of Health, Bethesda, MD, USA).

Data analysis and statistical methods

Data were expressed as the mean ± SEM or mean ± SD as indicated. Significance was assessed using one-way analysis of variance (ANOVA) followed by the Tukey–Kramer test using GraphPad Prism version 5. $p<0.05$ was considered significant (*), $p<0.01$ very significant (**).

Mass spectrometry analysis

The iPSCs were lysed in 1% SDS and the lysates were processed by using the FASP protocol as previously published [19]. Briefly, the cell lysates were sonicated, detergents removed by sequential washes in spin columns and proteins digested with trypsin. The peptides were analyzed on Q-Exactive Mass Spectrometer as previously described [20]. The proteins were identified and quantified with the MaxQuant 1.5 software suite by searching against the human uniprot database, with N-terminal actylation and methionine oxidation as variable modification and a FDR of 0.01. Mass accuracy was set a 4.5 ppm for the MS and 20 ppm for the MS/MS. LFQ was performed by MaxLFQ as described [21]. One-way ANOVA was carried out to compare Rapamycin treated samples with control iPSCs. The mean expression levels (M) and standard error of means (SEM) were quantified, and folds of changes in the treated samples were calculated against the control iPSCs (set as 1). $p<0.05$ was considered statistically significant. A total of 220 proteins which were significantly altered after Rapamycin treatment were analyzed by the STRING program for pathway using GO Biological processes and GO cellular components.

Results

Autophagy is a prominent feature of reprogramming cells and stable iPSCs

The autophagy-lysosome and ubiquitin-proteasome systems are the two major pathways that cells employ to selectively target long-lived and misfolded proteins, protein aggregates, damaged mitochondria, or unwanted cytoplasmic components and organelles [22]. We observed large autophagic vacuoles in the majority of cells during early reprogramming (red arrowheads, Figure 1A). In young passages of stable iPSCs, autophagic vacuoles were abundantly present but reduced in size (red arrowheads, Figure 1B). However, large autophagic vacuoles were absent in parental fibroblasts (Figure 1F). TEM revealed the presence of lysosomal structures (blue arrowheads, Figure 1E,I) in iPSCs. Structures of endosomal/lysosomal nature with double

membranes were clearly evident under high magnification, which were filled with an array of cell debris and organelles (Figure 1J-L).

Double immunofluorescence staining was carried out with anti-LC3B (an autophagy marker) and anti-LAMP1 (a major component of lysosomal membrane). In fibroblasts, fine dots of LC3B staining (green, Figure 1G) were observed and most of them were not colocalized with LAMP1 (red, Figure 1G). Similar to fibroblasts, small dots of LC3B staining were observed in iPSC culture which were not co-localized with LAMP1. However, strong LC3B staining appeared in large vacuoles (green, Figure 1C) which co-localized with anti-LAMP1 staining, which could represent different status of LC3B activity. The control double staining were performed with anti-Syntaxin 6, a marker for Golgi membrane and MitoGreen for mitochondria (Figure 1D,H). As anticipated, they were no colocalization in either iPSCs (Figure 1D) or fibroblasts (Figure 1H). These data therefore demonstrate that large autophagic vacuoles are a characteristic feature of iPSCs which harbor both LC3B-II and LAMP1.

iPSCs exhibit higher abundance of LC3B-II than parental fibroblasts

Next we compared iPSCs with parental fibroblasts from 4 independent donors by both immunocytochemtry (Figure 2a-D') and immoblotting (Figure 2E-G). The immunofluorescence study showed brighter basal LC3B-II staining in iPSCs (Figure 2A-D) than in parental fibroblasts (Figure 2a-d). Rapamycin (100nM) induced autophagy in both iPSCs (Figure 2A'-D') and fibroblasts (Figure 2a'-d'). Quantification of the immunoblots (Figure 2E) showed 2.55-fold higher basal LC3B-II in the iPSCs than that in parental fibroblasts (Figure 2F, $p<0.01$, n=4). After one day of Rapamycin induction at 100 nM, the LC3B-II was also 2.23-fold higher in the iPSCs than in fibroblasts (Figure 2G, $p<0.05$, n=4). Overall, these data show that autophagy is highly active in human iPSCs and is Rapamycin-inducible. Both the basal and induced autophagy are significantly higher in iPSCs than in dermal fibroblasts.

High basal levels of autophagy components are expressed in iPSCs

To further address the autophagy activity during iPSC maintenance, we determined basal expression levels of 10 autophagy members involving different steps of autophagy. Autophagy is repressed by the mTOR and activated by Rapamycin. ULK1/2 are activated in a ULK1/2-Atg13/101-FIP200 complex [23-24], which subsequently activates PI3K CIII complex (consisting of BECLIN-1, AMBRA, VPS34/15 and ATG14) and stimulates phagophore formation. ATG12 then conjugates with ATG5/16 and form phagophore [25]. ATG4/7/3 then converts LC3B-I to LC3B-II to form autophagic vacuole [17,22,26-27]. We extracted proteins from 12 iPSC lines derived from 10 independent donors (Figure 3), and carried out immunoblotting with antibodies against AMPKα, ULK1, ULK2, ATG13, ATG101, BECLIN-1, ATG3, ATG5, ATG12 and LC3B. Relative protein abundance was quantified against house-keeping proteins. AMPKα, BECLIN-1 ATG12, ATG13 and ULK1 were shown to be highly expressed in iPSCs, whereas ATG3, ATG101 and ULK2 were less abundant. No significant difference was detected among different lines for each component, but high levels of LC3B-II were detected in all iPSCs line (Figure 3A and 3C). To further evaluate the difference between iPSCs and fibroblasts, we investigated ATG5 and ATG12 expression among three fibroblast lines and 5 iPSC lines. The iPSCs were consistently showed to have much higher ATG5/ATG12 expression compared to fibroblasts (Figure 3H). These data demonstrate that most autophagy components are abundantly expressed in iPSCs.

Rapamycin induces iPSC autophagy in concentration- and time-dependent manners

To determine if iPSC maintenance might benefit from upregulated autophagy, we investigated the dosage effect of Rapamycin on phosphorylated ULK1, p70S6K, and the autophagy indicator - ratio of LC3B-II/I. Both ULK1 and p70S6K are serine/threonine kinases and targets of mTOR.

p70S6K is a major regulator of translation and phosphorylated by mTOR [28-30], whereas ULK1 is an initiator of autophagy.

We treated iPSCs with 0, 1, 10, 100, 200 or 300 nM of Rapamycin for 4 days, and observed a dose-dependent reduction in p70S6K phosphorylation (Figure 4I). The most significant reduction was achieved with 100-300 nM (Figure 4K). In contrast, LC3B-II (Figure 4J) and p-ULK1 (Figure 4L) were enhanced in a dose-dependent manner, and the maximal increase was observed at 200 nM of Rapamycin ($p<0.01$). Similarly, immunostaining detected higher levels of LC3B-II expression in 200 nM Rapamycin-induced cells (Figure 4A-D).

We then treated iPSCs with 200 nM of Rapamycin for 1, 3 and 6 days, observed significantly clustered LC3B-II staining after 3 days of Rapamycin treatment, and showed a time course-dependent activation of autophagy (Figure 4E-H). This was different from fibroblasts, in which the total LC3B was increased by 24 hrs of Rapamycin treatment, whereas the LC3B-II remained relatively constant (supplement Figure 1). These data demonstrate that autophagy can be markedly activated by Rapamycin in iPSCs.

Rapamycin attenuates Bafilomycin-induced iPSC death

Bafilomycin A1 is an inhibitor of lysosome degradation by blocking the final stage of autophagy, fusion of autophagosomes with lysosome (31-32). We treated iPSCs with 0, 5, 50, 100 nM of bafilomycin A1 for 24 or 48 hrs, with or without 200nM Rapamycin. Bafilomycin A1 was shown to induce iPSC death in concentration/time dependent manners. iPSC morphology was significantly altered after 24 hr of Bafilomycin treatment at 50 nM (Figure 5) but not at 5 nM (Figure 5B). At 100 nM, Bafilomycin markedly induced iPSC death in 24 hrs, leading to grossly reduced cell density after 48 hrs (Figure 5E). Addition of 200 nM Rapamycin significantly attenuated Bafilomycin-induced cell death, improved iPSC survival and increased iPSC cell density at 48 hrs Bafilomycin treatment (Figure 5G).

Western blotting showed that Bafilomycin enhanced both LC3B-I and -II bands by blocking basal autophagic flux. Rapamycin induced LC3B expression and caused a shift from LC3B-I to the LC3B-II (Figure 5H-I). Treatment of iPSCs with both Rapamycin and bafilomycin A1 increased conversion of LC3B-II from LC3B-I similar to Rapamycin treatment alone, thereby attenuated bafilomycin-induced cell death (Figure 5C-D). These data further strengthen the importance of autophagy in iPSCs, as blockage of fusion of autophagosomes with lysosome rapidly induces iPSC death. Meanwhile addition of Rapamycin significantly improves the iPSC survival.

Prolonged treatment with Rapamycin induces formation of uniform aggregates

We next cultured iPSCs in geltrex-coated dishes in the presence of 200 nM of Rapamycin and examined the long-term effects on the maintenance of iPSCs. We first noticed the following morphological changes: (1) the peripheral cells of the iPSC colonies first started to elongate (Figure 6D) after 3 days, and cells at the edge produced an unknown matrix which formed a firm line at the border of colony after 6 days to limit iPSC colony expansion sideway (arrowheads, Figure 6F-G); (2) Rapamycin altered iPSC cell junctions, and cell borders became more obvious after 2 days of treatment (Figure 6C-D); and (3) iPSCs continued to proliferate in the central areas of colonies, together with the limitation to expand sideway and reduced cell-cell contacts, round EB-like spheres were formed and detached from the culture dish before and after 6 days of Rapamycin treatment (*, Figure 6E-F).

The average aggregate size at 6 days was 64793±18779 μm^2 (n=13). The round spheres continued to detach and grow after 9 days of treatment, and reached the sizes of 112251±17422 (002V, n=8), 104640±27265 (JOM, n=13), 105381±13468 μm^2 (LV1, n=7) in three independent iPSC lines, respectively. However, the control EBs resulted from the cut-and-paste method varied significantly in shape and sizes (Figure 7F-H). They were 52328±25518 (002V, n=10); 80518±77708 (JOM, n=20); 75652±51944 μm^2 (LV1, n=22), respectively, and displayed

consistently large variation (SD) in sizes within each line (Figure 7B). These data show that high concentrations of Rapamycin treatment can induce iPSC detachment and spontaneous formation of uniformly sized aggregates.

Rapamycin treatment accelerates differentiation of human iPSCs

To determine the nature of the floating spheres resulting from Rapamycin treatment, we extracted proteins from the aggregates and compared them with EBs generated *via* the cut-and-paste method by immunoblotting with three germ layer markers of α-fetoprotein (AFP for endoderm), α-smooth muscle actin (ASM for mesoderm), and βIII tubulin (TUJ1 for ectoderm), together with autophagy marker LC3B-II (Figure 8A). The expression of these marker proteins was 2~3 fold higher in the Rapamycin-induced spheres (Figure 8A-C).

To examine differentiation potential of aggregates, we plated them out for spontaneous differentiation and compared with EBs made mechanically. Cells with neuronal morphology appeared after 3 days without neuronal induction (Figure 8J-L), and many were stained positive for neural stem cell marker NESTIN (Figure 8M). After 5 days of spontaneous differentiation, we carried out immunocytochemical staining with AFP, ASM, TUJ1, and obtained significantly higher proportions of cells positive for these makers in cells derived from Rapamycin-induced spheres (Figure 8G-I), compared with cells differentiated from the conventional EBs (Figure 8D-F). To illustrate mechanism(s) of Rapamycin-induced iPSC differentiation, we investigated NANOG expression after 4 days of treatment by immunoblotting (Figure 8L). Rapamycin was shown to down-regulate NANOG expression in a concentration-dependent manner, and significant reductions were detected at 100 nM ($p<0.05$), 200 nM ($p<0.01$) or 300 nM of Rapamycin treatment ($p<0.01$, Figure 8M). These data suggest that Rapamycin-induced spheres are similar to conventional EBs in pluripotency of differentiation, they are non-*biased* in

differentiating into three lineages, but differentiate in an accelerated pace, in association with down-regulated NANOG expression during EB formation.

Rapamycin regulates adherens junctions and actin cytoskeleton in human iPSCs

To identify potential molecular mechanisms associated with Rapamycin-induced iPSC detachment, we performed quantitative mass spectrometry analysis with proteins extracts from control iPSCs and iPSCs treated with 50, or 100 nM of Rapamycin for 3, 6, 9 days respectively (n=3 for each). A total of 6145 proteins were quantitatively identified, and 220 proteins were identified by statistical analyses, which were systematically altered at different time points and at both Rapamycin concentrations (One-way ANOVA, two-tailed, $p<0.05$). Gene ontology (GO) analyses of the 220 targets with the STRING database revealed that adherens junctions (17 hits, $p=6.49\text{x}10^{-6}$) and actin cytoskeleton (9 hits, $p=0.022$) were significantly enriched in the Rapamycin-treated cells (Figure 9), which integrated into an interactive network (Figure 9F).

Of the 17 adherens junction molecules, 9 (ACTN4, BSG, EPHA2, EZR, FLNB, PDLIM1, PPIA, SHROOM3, RPLP0) were down-regulated, and 8 (ABI2, GSN, ACTR3, ARF6, RALA, RPL7A, RPL19, RPL27) were up-regulated (Figure 9A-C). Of the 9 actin cytoskeleton associated proteins, 6 (ACTN4, CGN, EZR, FGD4, SERPINA3, TTN) were down-regulated and 3 (CTTNBP2NL, GSN, SEPT11) were up-regulated (Figure 9D-E). In consistent with the morphological changes, these data suggest that alterations of adherens junctions and cytoskeleton are the key pathways in Rapamycin-induced iPSC behavior.

Discussion

Autophagy is a cellular mechanism to maintain minimal cell activity for viability in response to nutrient limitations and cell stress, by degrading and recycling cytoplasmic proteins and

subcellular organelles *via* the fusion of a double-membrane-bound vesicle, autophagosome, with lysosome [17,33]. Autophagy plays an essential role in cellular reprogramming and basal level of autophagy increases in aging human skin fibroblasts, which may affect to different reprogramming efficiency [34]. It appears there is no co-relation with sex (all male) or age (4-20-year) in the fibroblast lines we have used, but with heath status, which requires validation in larger sample sets. In this study we demonstrate abundant presence of large autophagic vacuoles in early fibroblast reprogramming and smaller ones during the iPSC maintenance. We show high basal level of key components of autophagy in 12 iPSC lines derived from 10 independent donors, and prolonged Rapamycin treatment resulted spontaneous formation of uniformed sized EBs with accelerated differentiation pace.

In previous studies, lack of autophagy components of Atg3, or Atg5 or Atg7 was shown to render MEF cells defective in iPSC colony formation [15], and lack of two different autophagy genes, *atg5* and *beclin1*, displayed a defect in EB formation during development [35]. The reprogramming was entirely blocked also in *Tsc2*$^{-/-}$ somatic cells with hyperactivated mTOR activity which suppressed autophagy [14]. Subtle tuning of the mTOR activity with inhibitors, i.e. 0.3-1 nM Rapamycin or 0.1 nM PP242 was found to increase reprogramming efficiency [18]. Mechanistically, the reprogramming factor Sox2 could bind to mTOR promoter and repress mTOR expression and activate autophagy [15]. These data together showed that reduced mTOR activity and elevated Autophagy were required during cellular reprogramming, which is consistent with our observation that abundant large autophagic vacuoles are present in early fibroblast reprogramming, which become smaller during the subsequent passaging.

A balanced autophagy and mTOR activity is also essential for the maintenance and differentiation of pluripotent stem cells. Human ES cells were previously shown to have a tight regulation of the mTOR signaling to mediate protein translation for maintaining the pluripotent status [36]. Activation of p70S6K, a mTOR downstream factor, was shown to induce

differentiation of human ES cells [36], whereas inhibition of mTOR autophosphorylation by 20 nM Rapamycin was reported to disrupt p70S6K-mediated translation, but not to alter cell viability or expression of the pluripotency markers [37]. In contrast, the mTOR was necessary for growth and proliferation of early mouse embryos and ES cells, and disruption of the mouse mTOR gene prohibited ES cell development [38-39]. Interestingly, 100nM Rapamycin was previously shown to reduce the size and rate of EB formation in human amniotic fluid stem cells [40]. This was different from our study that high concentration of Rapamycin induced EB formation in iPSCs. Inhibition of the mTOR activity with high concentrations of Rapamycin also greatly impaired somatic cell reprogramming [14], and 100 nM Rapamycin was used to primer hepatocyte differentiation of iPSCs prior to Activin A induction [41]. This is consistent with our data that Rapamycin down-regulates NANOG expression in a concentration dependent manner and accelerates iPSC differentiation.

To uncover Rapamycin pathways in iPSCs, we carried out quantitative mass spectrometry. The STRING Gene Ontology analyses revealed that actin cytoskeleton and adherens junctions were the integrated pathways regulated by Rapamycin. For example, ACTN4, BSG, CGN, EPHA2, EZR, FGD4, FLNB, PDLIM1, PPIA, SHROOM3, RPLP0, SERPINA3 and TTN were significantly down-regulated, whereas ABI2, CTTNBP2NL, GSN, ACTR3, ARF6, RALA, RPL7A, RPL19, RPL27 and SEPT11 were up-regulated.

Actin is critical for cell shape, adhesion and migration. The dynamics of actin cytoskeleton are modulated by Rapamycin targets of SHROOM3, EZR and GSN. For example, SHROOM3 is required for the apical localization of F-actin/myosin II [42]. EZR links the plasma membrane to actin and is involved in adhesion and migration. Inhibition of EZR expression reduced adhesiveness in colorectal cancer cells [43]. GSN knockdown decreased cell viability and tumor cell invasion, whereas GSN overexpression correlates with proliferative and invasive capacities [44]. BSG promotes cell–cell adhesion, and its down-regulation altered actin/Spectrin network

[45]. Therefore, reduced expression of SHROOM3, EZR and BSG in the Rapamycin-treated iPSCs is in line with reduced cell adhesion in the literature.

ACTN4, FLNB, PDLIM1 are actin-binding proteins. ACTN4 is concentrated at sharp extension and at the edge of cell clusters [46], and FLNB regulates direct communication between the cell membrane and cytoskeletal network [47]. PDLIM1 function as an adapter to recruit other LIM-interacting proteins to the cytoskeleton, and suppression of PDLIM1 resulted in cell spreading and the loss of stress fibers and focal adhesions [48]. In addition, ACTR3 is also essential to cell shape and motility, and is an ATP-binding component of the ARP2/3 complex, which regulates actin polymerization. The complex can be activated by ABI, and knockdown of ABI markedly inhibits cell-cell junctions [49]. Therefore, Rapamycin-induced changes in the expression of ACTN4, ACTR3, FLNB and PDLIM1 are also likely to affect actin cytoskeleton.

Some of Rapamycin targets are GTPase activity-related, such as downregulated EPHA2 and upregulated ARF6 and RALA. GTPases are involved in cell adhesion migration and oncogenic transformation. For example, EphA2 is a transmembrane receptor tyrosine kinase activating and prompts cells to round up and detach from their neighbors [50]. RALA is a small GTPase and constitutively active RALA promotes anchorage-independent growth signaling [51]. ARF6 is a small GTPase to balance with RAB35 GTPase by cells during cell migration and adhesion. Increased ARF6 activity from RAB35 knockdown enhances cadherins accumulation and reduces cell–cell adhesion. The loss of RAB35, However, correlates with enhanced cell migration [52]. Therefore, reduced EPHA2 and increased ARF6 and RALA expression may also contribute to Rapamycin-induced iPSC detachment. Together these data showed that Rapamycin regulates an array of adherens junctions and actin modifying molecules, which collectively alters iPSC adhesion.

Conclusions

In this study, we demonstrate that autophagy is a prominent feature of reprogramming cells and stable iPSCs. The basal level of autophagy is universally present among human iPSC lines, which is significantly higher than parental fibroblasts. Block of autophagy by Bafilomycin induces iPSC death. Rapamycin activates autophagy in concentration- and time-dependent manners and attenuate Bafilomycin toxicity in iPSCs. Prolonged Rapamycin treatment induces cell detachment and formation of uniformly sized EBs from human iPSCs, with altered expression of adherens junctions and actin modifying molecules. The Rapamycin downregulates NANOG expression, induces EBs formation and accelerates cell differentiation into three germ layer lineages. This findings are significant in two-fold. Firstly, the 3D microenvironment including shape and sizes of EBs can affect differentiation. The iPSCs are supersensitive to enzyme dissociation and therefore the "hanging drop" technique is difficult to apply, despite it was available to generate uniform EBs from ES cells over 20 years ago. Rapamycin may therefore assist generation of uniformly sized EB with round shape which may reduce the heterogeneity of the end cell types. Secondly, differentiation of mature and functional cell types from human iPSCs is time-consuming, and the accelerated differentiation associated with Rapamycin treatment is promising in shortening the differentiation duration. Rapamycin, therefore, may find its application in assistance of overcoming the challenges associated with phenotypic characterization, drug discovery and cell replacement therapy for neurological disorders.

Declarations

Abbreviations

AFP, α-fetoprotein; ANOVA, one-way analysis of variance; ASM, α-smooth muscle actin; *ATG*s, Autophagy-Related Genes; EBs, embryoid bodies; ER, endoplasmic reticulum; ES, embryonic stem; iPSCs, induced pluripotent stem cells; LC3I, microtubule-associated proteins 1A/1B light chain 3-I; MEF, mouse embryonic fibroblasts; mTOR, mammalian target of the Rapamycin; NaB, sodium butyrate; PE, phosphatidylethanolamine; PVDF, polyvinylidene difluoride; SEM, standard error of means; TEM, transmission electron microscopy; TUJ1, βIII tubulin.

Ethical approval and consent to participate

The iPSC study was carried out in compliance with the ethical approval of the Clinical Research Ethics Committee, Galway University Hospitals, and informed consent was obtained from all participants prior to skin biopsy donation.

Consent for publication

Informed consent was obtained from volunteers for disclosure of the research data anonymously.

Availability of supporting data

Not applicable.

Competing interests

Authors declare no potential conflicts of interest.

Funding

This work was supported by Science Foundation Ireland (SFI), Strategic Research Cluster (SRC), grant No. SFI: 09/SRC B1794 and 09/SRC/B1794s1, SFI Investigator Programme 13/IA/1787, SFI TIDA program 14/TIDA/2258; NUI Galway Grant RSU002.

Authors' contributions

A.S. performed the majority of the experiments; K.M. and A.K made iPSC lines, K.M. contributed IC/WB data during revisions; M.J.D and T.K contributed additional iPSC lines; J.K and V.M in patient recruitment; K.T and P.D participated in microscopic characterization; K.D.C did independent treatment for proteomics, A.v.K and A.G-M performed proteomics; F.B., and T.O oversaw the project and edited manuscript; A.S and S.S designed the experiments, analyzed the data and wrote the manuscript.

Acknowledgements

The authors acknowledge the facilities and technical assistance from the Centre for Microscopy & Imaging at the National University of Ireland Galway (www.imaging.nuigalway.ie), a facility that is funded by NUIG and the Irish Government's Programme for Research in Third Level Institutions, Cycles 4 and 5, National Development Plan 2007-2013.

Authors' information

A.S: BSc, MSc, PhD, postdoctoral researcher, Regenerative Medicine Institute, School of Medicine, NUI Galway, Ireland, and now a Lecturer at Chulabhorn International College of Medicine, Thammasat University, Thailand.

K.M.: BSc, MSc, PhD, postdoctoral researcher, Regenerative Medicine Institute, School of Medicine, NUI Galway, Ireland.

A.v.K.: BSc, MSc, PhD, Research Fellow, Systems Biology Ireland, University College Dublin, Ireland, and now Mass-spectrometry Manager at Edinburgh University, UK.

A.G-M.: BSc, MSc, PhD, Lab Manager, Systems Biology Ireland, Conway Institute, UCD, Ireland.

A.K.: MSc, Regenerative Medicine Institute, School of Medicine, NUI Galway, Ireland.

K.T.: BSc, PhD, Postdoctor Microscopy Facility Scientist**,** School of Medicine, NUI Galway, Ireland.

K.D.C.: MSc, PhD, Postdoctor, Regenerative Medicine Institute, School of Medicine, NUI Galway, Ireland.

J.K., MB, MD, Consultant Haematologist, Senior Lecturer, Galway University Hospital.

V.M.: MSc, PhD, Clinical Manager , HRB Clinical Research Facility, NUI Galway, Ireland.

P.D.: BSc, PhD, Head of Anatomy, Centre for Microscopy and Imaging, School of Medicine, NUI Galway, Ireland.

M.J.D.: MD, PhD, MRC Clinical Research Fellow at MRC center for Regenerative Medicine, The University of Edinburgh, UK.

T.K.: BSc, MSc, PhD, Principal Investigator, MRC center for Regenerative Medicine, The University of Edinburgh, UK.

F.B., BSc, MSc, PhD, Professor of Cellular Therapy and Scientific Director of the Regenerative Medicine Institute, School of Medicine, NUI Galway, Ireland.

T.O.: MB BCh BAO , MD, PhD, Director of the Regenerative Medicine Institute, Dean of the College of Medicine and Life Sciences, NUI Galway, Ireland.

S.S.: BSc, MSc, PhD, Professor of Fundamental Stem Cell Biology, Regenerative Medicine Institute, School of Medicine, NUI Galway, Ireland.

References

1. Takahashi K, Yamanaka S. Induction of pluripotent stem cells from mouse embryonic and adult fibroblast cultures by defined factors. Cell. 2006;126:663-76.

2. Chu A, Caldwell JS, Chen YA. Identification and characterization of a small molecule antagonist of human VPAC(2) receptor. Mol Pharmacol. 2010;77:95-101.
3. Dolmetsch R, Geschwind DH. The human brain in a dish: the promise of iPSC-derived neurons. Cell. 2011;145:831-34.
4. Bellin M, Marchetto MC , Gage FH, Mummery CL. Induced pluripotent stem cells: the new patient? Nat Rev Mol Cell Biol. 2012;13:713-26.
5. Chailangkarn T, Acab A, Muotri AR. Modeling neurodevelopmental disorders using human neurons. Curr Opin Neurobiol. 2012; 22:785-90.
6. Kim KY, Jung YW, Sullivan GJ, Chung L, Park IH. Cellular reprogramming: a novel tool for investigating autism spectrum disorders. Trends Mol Med. 2012;18:463-71.
7. Nakano T, Ando S, Takata N, Kawada M, Muguruma K, Sekiguchi K, et al. Self-formation of optic cups and storable stratified neural retina from human ESCs. Cell Stem Cell. 2012;10:771-85.
8. Sasai Y, Eiraku M, Suga H. In vitro organogenesis in three dimensions: self-organising stem cells. Development. 2012;139:4111-21.
9. Lancaster MA, Renner M, Martin CA, Wenzel D, Bicknell LS, Hurles ME, et al. Cerebral organoids model human brain development and microcephaly. Nature. 2013;501:373-79.
10. Hwang YS, Chung BG, Ortmann D, Hattori N, Moeller HC, Khademhosseini A. Microwell-mediated control of embryoid body size regulates embryonic stem cell fate via differential expression of WNT5a and WNT11. Proc Natl Acad Sci (USA). 2009; 106:16978-83.
11. Hu BY, Du ZW, Zhang SC. Differentiation of human oligodendrocytes from pluripotent stem cells. Nat Protoc. 2009; 4:1614-22.

12. Shi Y, Kirwan P, Livesey FJ. Directed differentiation of human pluripotent stem cells to cerebral cortex neurons and neural networks. Nat Protoc. 2012;7:1836-46.

13. Liu Y, Liu H, Sauvey C, Yao L, Zarnowska ED, Zhang SC. Directed differentiation of forebrain GABA interneurons from human pluripotent stem cells. Nat Protoc. 2013; 8:1670-79.

14. He J, Kang L, Wu T, Zhang J, Wang H , Gao H, et al. An elaborate regulation of Mammalian target of Rapamycin activity is required for somatic cell reprogramming induced by defined transcription factors. Stem Cells Dev. 2012;21:2630-41.

15. Wang S, Xia P, Ye B, Huang G, Liu J, Fan Z. Transient activation of autophagy via Sox2-mediated suppression of mTOR is an important early step in reprogramming to pluripotency. Cell Stem Cell. 2013;13:617-25.

16. Ohsumi Y. Molecular dissection of autophagy: two ubiquitin-like systems. Nat Rev Mol Cell Biol. 2001; 2:211-16.

17. Glick D, Barth S, Macleod KF. Autophagy: cellular and molecular mechanisms. J Pathol. 2010;221:3-12.

18. Chen T, Shen L, Yu J, Wan H, Guo A, Chen J, et al. Rapamycin and other longevity-promoting compounds enhance the generation of mouse induced pluripotent stem cells. Aging Cell. 2011;10:908-11.

19. Wiśniewski JR, Zougman A, Nagaraj N, Mann M. Universal sample preparation method for proteome analysis. Nat Methods. 2009; 6:359-62.

20. Farrell J, Kelly C, Rauch J, Kida K, García-Muñoz A, Monsefi N, et al. HGF induces epithelial-to-mesenchymal transition by modulating the mammalian hippo/MST2 and ISG15 pathways. J Proteome Res. 2014; 13:2874-86.

21. Cox J, Hein MY, Luber CA, Paron L, Nagaraj N, Mann M. Accurate proteome-wide label-free quantification by delayed normalization and maximal peptide ratio extraction, termed MaxLFQ. Mol Cell Proteomics. 2014; 13:2513-26.

22. Nixon RA. The role of autophagy in neurodegenerative disease. Nat Med. 2001; 19:983-97.

23. Klionsky DJ, Cregg JM, Dunn WAJr, Emr SD, Sakai Y, Sandoval IV, et al. A unified nomenclature for yeast autophagy-related genes. Dev Cell. 2003; 5:539-45.

24. Klionsky DJ. The molecular machinery of autophagy: unanswered questions. J Cell Sci. 2005; 118:7-18.

25. Sakoh-Nakatogawa M, Matoba K, Asai E, Kirisako H, Ishii J, Noda NN, et al. Atg12-Atg5 conjugate enhances E2 activity of Atg3 by rearranging its catalytic site. Nat Struct Mol Biol. 2013; 20:433-39.

26. Jaeger PA, Wyss-Coray T. All-you-can-eat: autophagy in neurodegeneration and neuroprotection. Mol Neurodegener. 2009; 4:16.

27. Alers S, Loffler AS, Wesselborg S, Stork B. Role of AMPK-mTOR-Ulk1/2 in the regulation of autophagy: cross talk, shortcuts, and feedbacks. Mol Cell Biol. 2012; 32:2-11.

28. Alessi DR, Kozlowski MT, Weng QP, Morrice N, Avruch J. 3-Phosphoinositide-dependent protein kinase 1 (PDK1) phosphorylates and activates the p70 S6 kinase in vivo and in vitro. Curr Biol. 1998; 8:69-81.

29. Pullen N, Dennis PB, Andjelkovic M, Dufner A, Kozma SC, Hemmings BA et al. Phosphorylation and activation of p70s6k by PDK1. Science. 1998; 279:707-10.

30. Weng QP, Kozlowski M, Belham C, Zhang A, Comb MJ, Avruch J. Regulation of the p70 S6 kinase by phosphorylation in vivo. Analysis using site-specific anti-phosphopeptide antibodies. J Biol Chem. 1998; 273:16621-29.

31. Yamamoto A, Tagawa Y, Yoshimori T, Moriyama Y, Masaki R, Tashiro Y. Bafilomycin A_1 prevents maturation of autophagic vacuoles by inhibiting fusion between autophagosomes and lysosomes in rat hepatoma cell line, H-4-II-E cells. Cell Struct Funct. 1998; 23:33-42.

32. Klionsky DJ, Elazar Z, Segllen PO, Rubinsztein DC. Does Bafilomycin A_1 block the fusion of autophagosome with lysosomes? Autophagy. 2008; 4:849-50.

33. Cecconi F, Levine B. The role of autophagy in mammalian development: cell makeover rather than cell death. Dev Cell. 2008; 15:344-57.

34. Demirovic D, Nizard C, Rattan SIS. Basal Level of Autophagy Is Increased in Aging Human Skin Fibroblasts In Vitro, but not in old Skin. PLoS one. 2015; 10:e0126546.

35. Qu X, Zou Z, Sun Q, Luby-Phelps K, Cheng P, Hogan RN, et al. Autophagy gene-dependent clearance of apoptotic cells during embryonic development. Cell. 2007; 128:931-46.

36. Zhou J, Su P, Wang L, Chen J, Zimmermann M, Genbacev O, et al. mTOR supports long-term self-renewal and suppresses mesoderm and endoderm activities of human embryonic stem cells. Proc Natl Acad Sci (USA). 2009; 106:7840-45.

37. Easley CA4th, Ben-Yehudah A, Redinger CJ, Oliver SL, Varum ST, Eisinger VM, et al. mTOR-mediated activation of p70 S6K induces differentiation of pluripotent human embryonic stem cells. Cell Reprogram. 2010; 12:263-73.

38. Gangloff YG, Mueller M, Dann SG, Svoboda P, Sticker M, Spetz JF, et al. Disruption of the mouse mTOR gene leads to early postimplantation lethality and prohibits embryonic stem cell development. Mol Cell Biol. 2004; 24:9508-16.

39. Murakami M, Ichisaka T, Maeda M, Oshiro N, Hara K, Edenhofer F, et al. mTOR is essential for growth and proliferation in early mouse embryos and embryonic stem cells. Mol Cell Biol. 2004; 24:6710-18.

40. Valli A, Rosner M, Fuchs C, Siegel N, Bishop CE, Dolznig H, et al. Embryoid body formation of human amniotic fluid stem cells depends on mTOR. Oncogene. 2010; 18;29(7):966-77.

41. Vosough M, Omidinia E, Kadivar M, Shokrgozar MA, Pournasr B, Aghdami N. Generation of functional hepatocyte-like cells from human pluripotent stem cells in a scalable suspension culture. Stem Cells Dev. 2013; 22:2693-705.

42. Plageman TFJr, Chung MI, Lou M, Smith AN, JHildebrand JD, Wallingford JB, et al. Pax6-dependent Shroom3 expression regulates apical constriction during lens placode invagination. Development. 2010; 137:405-15.

43. Hiscox S, Jiang WG. Ezrin regulates cell-cell and cell-matrix adhesion, a possible role with Ecadherin/b-catenin. J Cell Sci. 1999; 112:3081-90.

44. Deng B, Fang J, Zhang X, Qu L, Cao Z, Wang B. Role of gelsolin in cell proliferation and invasion of human hepatocellular carcinoma cells. Gene. 2015; 571:292-97.

45. Besse F, Mertel S, Kittel RJ, Wichmann C, Rasse TM, Sigrist SJ, et al. The Ig cell adhesion molecule Basigin controls compartmentalization and vesicle release at Drosophila melanogaster synapses. J Cell Biol. 2007; 177:843-55.

46. Honda K, Yamada T, Endo R, Ino Y, Gotoh M, Tsuda H, et al. Actinin-4, a novel actin-bundling protein associated with cell motility and cancer invasion. J Cell Biol. 1998; 140:1383-93.

47. Lu J, Lian G, Lenkinski R, De Grand A, Vaid RR, Bryce T, et al. Filamin B mutations cause chondrocyte defects in skeletal development. Hum Mol Genet. 2007; 16:1661–75.

48. Tamura N, Ohno K, Katayama T, Kanayama N, Sato K. The PDZ-LIM protein CLP36 is required for actin stress fiber formation and focal adhesion assembly in BeWo cells. Biochem Biophys Res Commun. 2007; 364:589-94.

49. Ryu JR, Echarri A, Li R, Pendergast AM. Regulation of cell-cell adhesion by Abi/Diaphanous complexes. Mol Cell Biol. 2009; 29:1735-48.

50. Sugiyama N, Gucciardo E, Tatti O, Varjosalo M, Hyytiäinen M, Gstaiger M, et al. EphA2 cleavage by MT1-MMP triggers single cancer cell invasion via homotypic cell repulsion. J Cell Biol. 2013; 201:467-84.

51. Balasubramanian N, Meier JA, Scott DW, Norambuena A, White MA, Schwartz MA. RalA-exocyst complex regulates integrin-dependent membrane raft exocytosis and growth signaling. Curr Biol. 2010; 20: 75-79.

52. Allaire PD, Seyed SM, Chaineau M, Seyed SE, Konefal S, Fotouhi M, et al. Interplay between Rab35 and Arf6 controls cargo recycling to coordinate cell adhesion and migration. J Cell Sci. 2003; 126:722-31.

Figure legends

Figure 1. Autophagy machinery is widely operated in iPSCs. (A) Images of cells were taken at day 15 of fibroblast reprogramming and large autophagic vauoles were arrowheaded. (B) Smaller autophagic vacuoles (arrowheaded) were observed in stable iPSC lines with daily change of culture medium. (C-D,G-H) Double immunofluorescence staining of iPSCs (C-D) and fibroblasts (G-H) was carried out with anti-LC3B for autophagy (C,G, green) and anti-LAMP1 for lysosome (C,G, red), Syntaxin 6 for Golgi membrane (D,H, red) and MitoGreen (D, H, green) for mitochondria, with counter-staining of DAPI (blue) for nuclei. Fluorescent images were acquired *via* confocal microscopy. Note that LC3B and LAMP1 are colocalized in iPSCs (C) but not in fibroblasts (G), whereas Syntaxin 6/MitoGreen are not colocalized as anticipated

(D,H). (E, I-L) Transmission electronic microscopic images showed a dead neucleus (*, A and E), lysosomal structures (blue arrowheads, E,I), and autophagic vacuoles (red arrowheads, J-L). Bars=20 µm in A-D and F-H; 10 µm in E and I; 500 nm in J-L.

.

Figure 2. iPSCs exhibit higher autophagy activity than parental fibroblasts. Fibroblasts (a-d, a'-d') and iPSCs (A-D, A'-D') derived from 4 independent donors were culture in the absence (-R) or presence (+R) of 100nM Rapamycin for 24 hours. The iPSCs showed higher basal staining of LC3B (A-D) than in parental fibroblasts (a-d). LC3B was highly induced by 100 nM of Rapamycin in iPSCs (A'-D'), with lower levels of induction in their respective fibroblasts (a'-d'). Fluorescent images were acquired *via* confocal microscopy. Bar=10 µm. (E) Immunoblots of the protein extracts from untreated (-R) or treated (+R) cells with anti-LC3B-II and anti-β-ACTIN. (F-G) The relative abundance of LC3B-II was quantified using ImageJ and data were presented with Mean ± SD. (F) The basal level of LC3B-II in the iPSCs was 2.55-fold higher than in parental fibroblasts (**, $p<0.01$, n=4). (G) Rapamycin-induced expression of LC3B-II in the iPSCs was also 2.23-fold higher than fibroblasts (*, $p<0.05$, n=4).

Figure 3. Wide expression of different autophagy components in independent iPSC lines. Proteins were extracted from iPSCs with daily renewal of culture medium. 15 µg of protein was loaded onto each lane. Lane a-l represents 12 independent iPSC lines from 10 donors (a, 33D6; b, JOM; c, LV1; d, LV2; e, LV3; f, 001CC1; g, NRXN1C1; h, 002V; I, 003V; j, SC126; k, SC128, l, SC132). (A-C) Immunoblotting was carried out with antibodies against LC3B-I, LC3B-II, BECLIN-1, AMPKα, ULK1, ULK2, ATG3, ATG12, ATG13, ATG101 and β-Actin. (D-G) The relative abundance of the proteins was quantified using ImageJ against β-Actin and data were presented with Mean ± SD. (H) Immunoblots were carried out to compare expression

of ATG5 and ATG 12 among 3 fibroblast lines (3x Fib.) and 5 iPSC lines (5xiPSCs) of healthy donors, showing higher ATG5 and ATG12 expression in iPSCs than that in fibroblasts.

Figure 4. Rapamycin induces autophagy in time- and concentration-dependent manners in iPSCs. iPSCs were maintained in 6-well plates and medium was renewed daily. Image of LC3B staining in panels A-D were taken from 4 days of Rapamycin treatment at 0, 10, 100 or 200 nM respectively, and image in panels E-H were sampled from 200 nM of Rapamycin treatment for 1, 3 and 6 days respectively, showing concentration- and time-dependent induction. (I) Proteins were extracted from iPSCs treated with Rapamycin at 0, 1, 10, 100, 200 or 300 nM for 4 days, and immunobloted with antibodies against LC3B, phosphorylated ULK1, phosphorylated p70 S6K or β-Actin. (J-L) The relative abundance of the LC3B-II/I ratios (J), p-p70S6K (K) and p-ULK1 (L) was quantified using ImageJ against a loading control β-Actin. Data were presented with Mean ± SEM, with * for $p<0.05$, and ** for $p<0.01$. Bars = 10μm in A-H.

Figure 5. Rapmycin attenuates Bafilomycin A1-induced iPSC death. iPSCs were treated with 0 (A), 5nM (B) , 50 nM (C) , 100 nM (D,E) of Bafilomycin for 24 (A-D) or 48 hours (E). Bafilomycin A1 induced cell death in a concentration dependent manner (A-D), leading to substantial cell loss after 48 hours at 100 nM (D). Addition of 200 nM Rapamycin attenuate Bafilomycin A1-induced cell death and maintained iPSC normal cell density (F,G). (H) Anti-ACTIN and Anti-LC3B immoblotting were carried out with iPSC lysates from control iPSCs (Con), or 24 hour of treatment with 200 nm of Rapmycin (Rap), or with 100 nM of Bafilomycin A1 (Baf) or with both (Rap+Baf). (I) The relative abundance of the LC3B-II/I ratios was quantified against a loading control β-ACTIN. Data were presented with Mean ± SEM, with * for $p<0.05$, and ** for $p<0.01$, n = 4. Bar=50 μm in A-B.

Figure 6. A time course of Rapamycin-induced cell detachment and EB formation. iPSCs were cultured in the presence of 200 nM Rapamycin. Bright field microscopic images were taken after 1 (B), 2 (C), 3 (D) and 6 (E-F) days of treatment. EB-like spheres were spontaneously formed after 6 days of Rapamycin treatment. Arrowheads in C, E and F indicated the border of the iPSC colonies which formed a line after day 6 to limit colony expansion sideway. (E) * indicated the areas of iPSC detachment, which were filled with a thin layer of iPSCs. (F) Four EB-like spheres of comparable size were captured in the fields. (G) Magnified view (4x) of the border area arrowheaded in image F. Bar=100 μm in A-D, 200 μm in E-F.

Figure 7. Rapamycin induces spontaneous formation of uniform sizes of EBs. (A-C) Images of floating spheres appeared after 9 days of Rapamycin treatment (200 nM) from 3 iPSC lines. (D-F) Images of EBs made after 9 days from "cut-and-paste" method. (G) The EB area sizes (μm^2) were quantified with ImageJ and data were presented with Mean ± SD. Note the round shape and uniform sizes of EBs from Rapamycin treatment (A-C), in contrast to irregular shape and sizes of EBs resulted from the same iPSC lines by mechanical method (D-F). Bar = 200 μm.

Figure 8. Rapamycin treatment accelerates differentiation of human iPSCs in association with decreased NANOG expression. (A) Proteins were extracted from Rapamycin-induced spheres and control EBs, and blotted with antibodies against LC3B, AFP, ASM, TUJ1 and β-ACTIN. (B) Relative protein expression was quantified against β-ACTIN, (C) compared between two methods, and presented as M ± SEM. Note a 2~3 fold increase of LC3B, AFP, ASM, and TUJ1 expression in Rapamycin-induced spheres. Rapamycin-induced spheres and control EBs were plated out for spontaneous differentiation for 3 days (J-K) or 5 day (D-I), and stained for NESTIN (M), TUJ1 (D, G), ASM (E, H), AFP (E, I). Note the presence of more immune-

positive cells in derivatives of Rapamycin-induced spheres (G-I) compared with cells differentiated from conventional EBs (E-F). (L) Proteins were extracted from iPSCs treated with Rapamycin at 0, 1, 10, 100, 200 or 300 nM for 4 days, and immunobloted with anti-NANOG, showing concentration-dependent reduction of NANOG expression after Rapamycin treatment. (M) Relative abundance of NANOG expression after 4 days of Rapamycin treatment. Bar = 100 µm in D-I; Bar = 50 µm in J-K. * for $p<0.05$, and ** for $p<0.01$.

Figure 9. Rapamycin regulates adherens junctions and actin cytoskeleton pathways in iPSCs. Three independent lines of iPSCs were maintained in mTeSR™ (con) or in the presence of 50 or 100nm Rapamycin for 3, 6 or 9 days. Proteins were harvested for Mass Spectrometry analyses. (A-E) The time course changes of protein expression (mean±SEM, n=3). * for $p<0.05$. (F) The molecular network for selected proteins whose expression was altered. The data show the network of interactions between adherens junctions and actin signaling by the STRING. The arrows indicated up- or down-regulation of the protein expression after Rapamycin treatment.

Supplemental Figure 1. Rapamycin induces LC3B expression in human fibroblasts. Three lines of human fibroblasts (F1, F2, F3) were treated without (-) or with (+) 100 nM Rapamycin overnight. The protein lysates were run of 15% SDS-PAGE and blotted with anti-LC3B and anti-GAPDH. Two bands of LC3B-I (16kD) and LC3B-II (14kD) were seen. Rapamycin is shown to induce LC3B-I expression after 24 hours of treatment.

Figure 1

Click here to download Figure ShenFig 1 R1 flat.tif

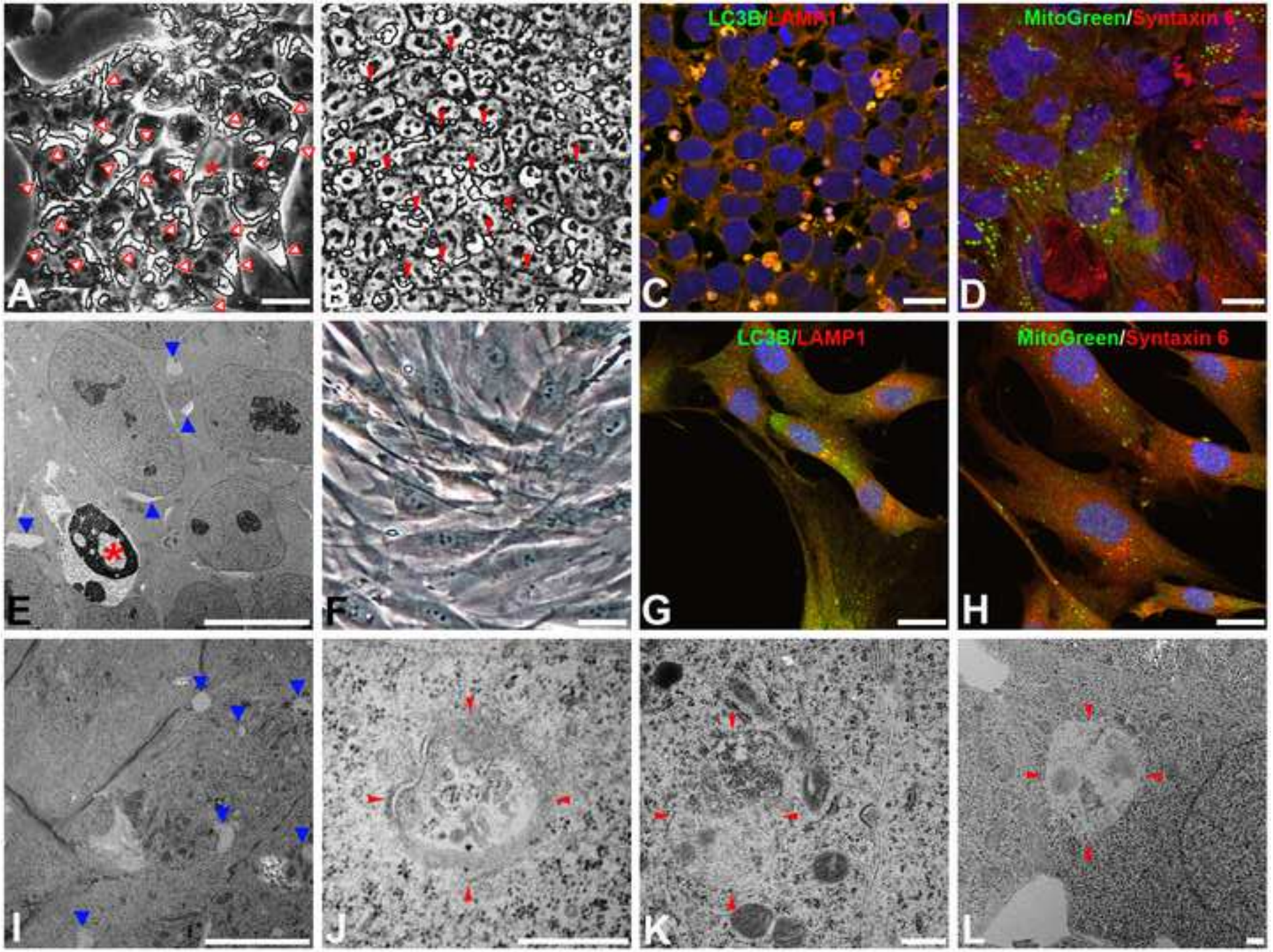

Figure 2

Click here to download Figure ShenFig 2 R1.tif

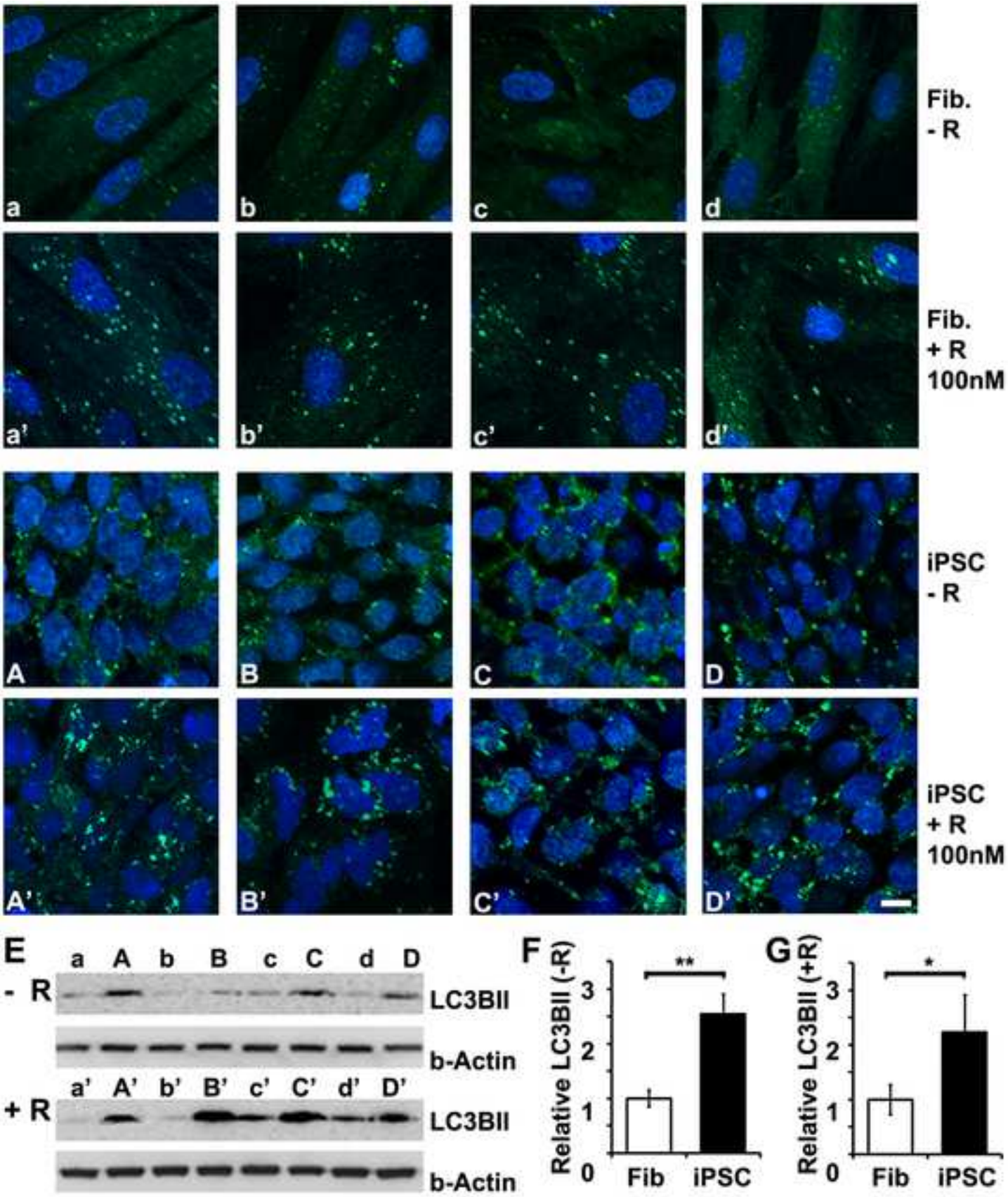

Figure 3

Click here to download Figure ShenFig 3 R1.tif

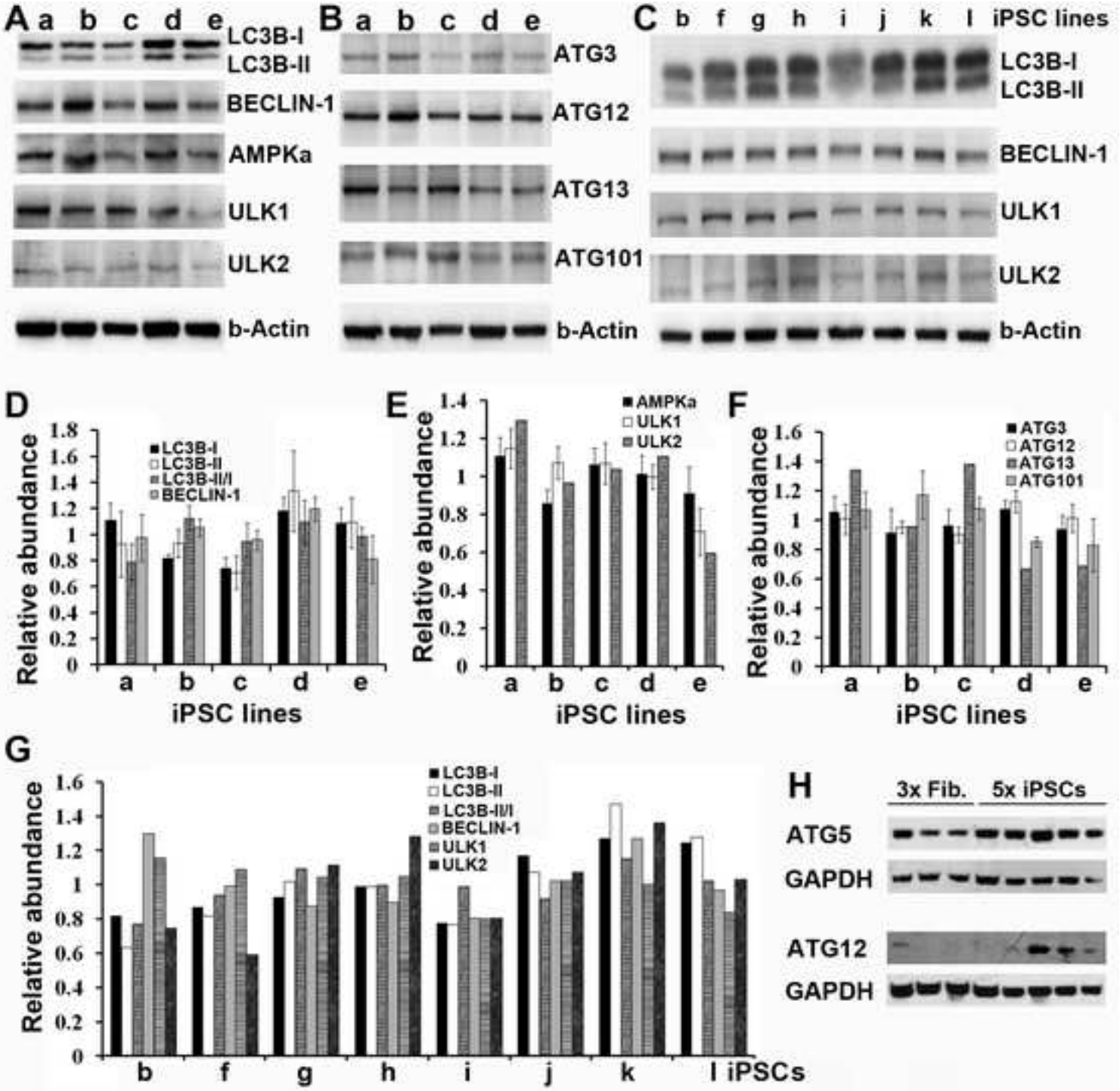

Figure 4

Click here to download Figure ShenFig 4 R1.tif

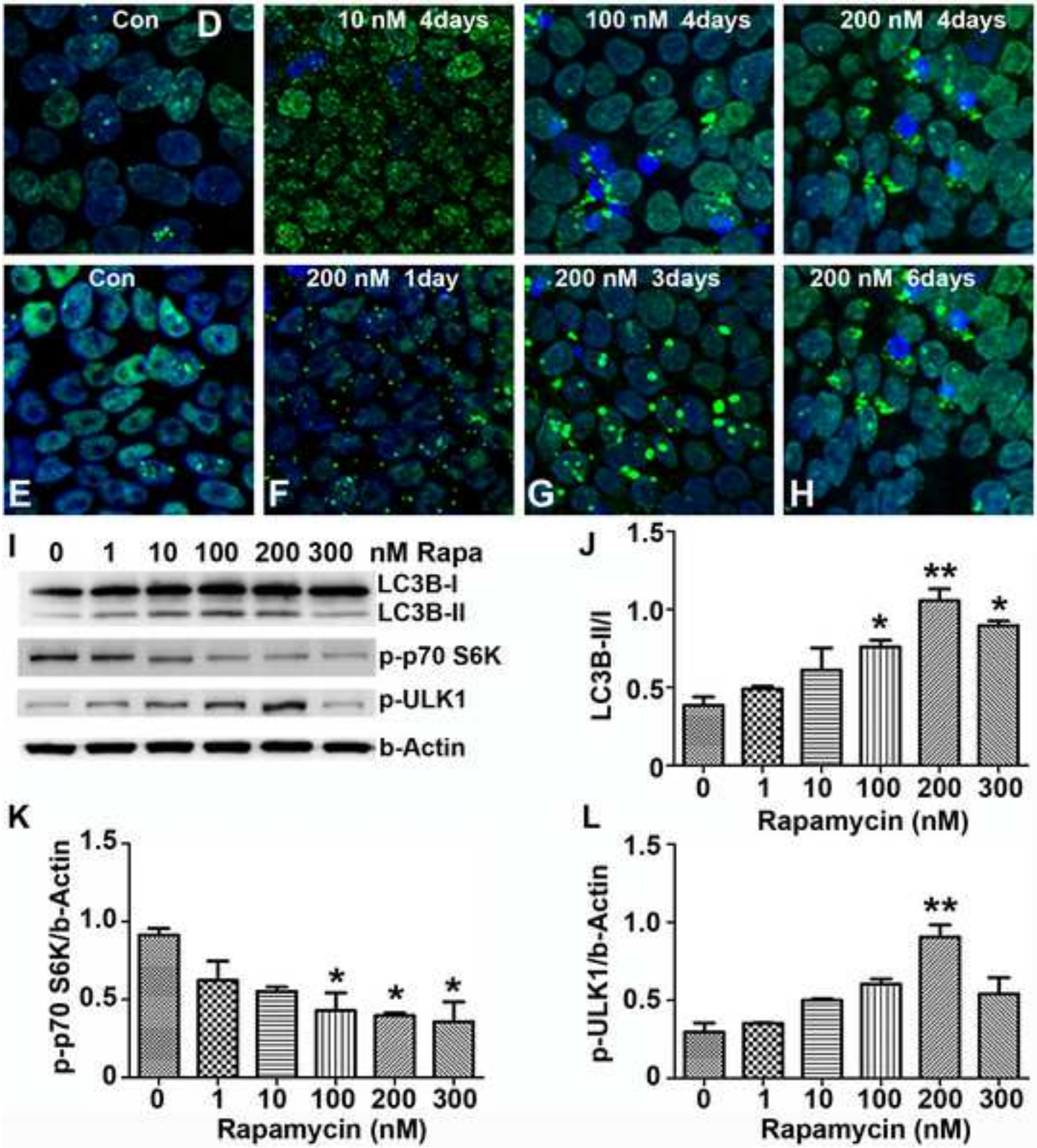

Figure 5

Click here to download Figure ShenFig 5 Baf+Rap R1.tif

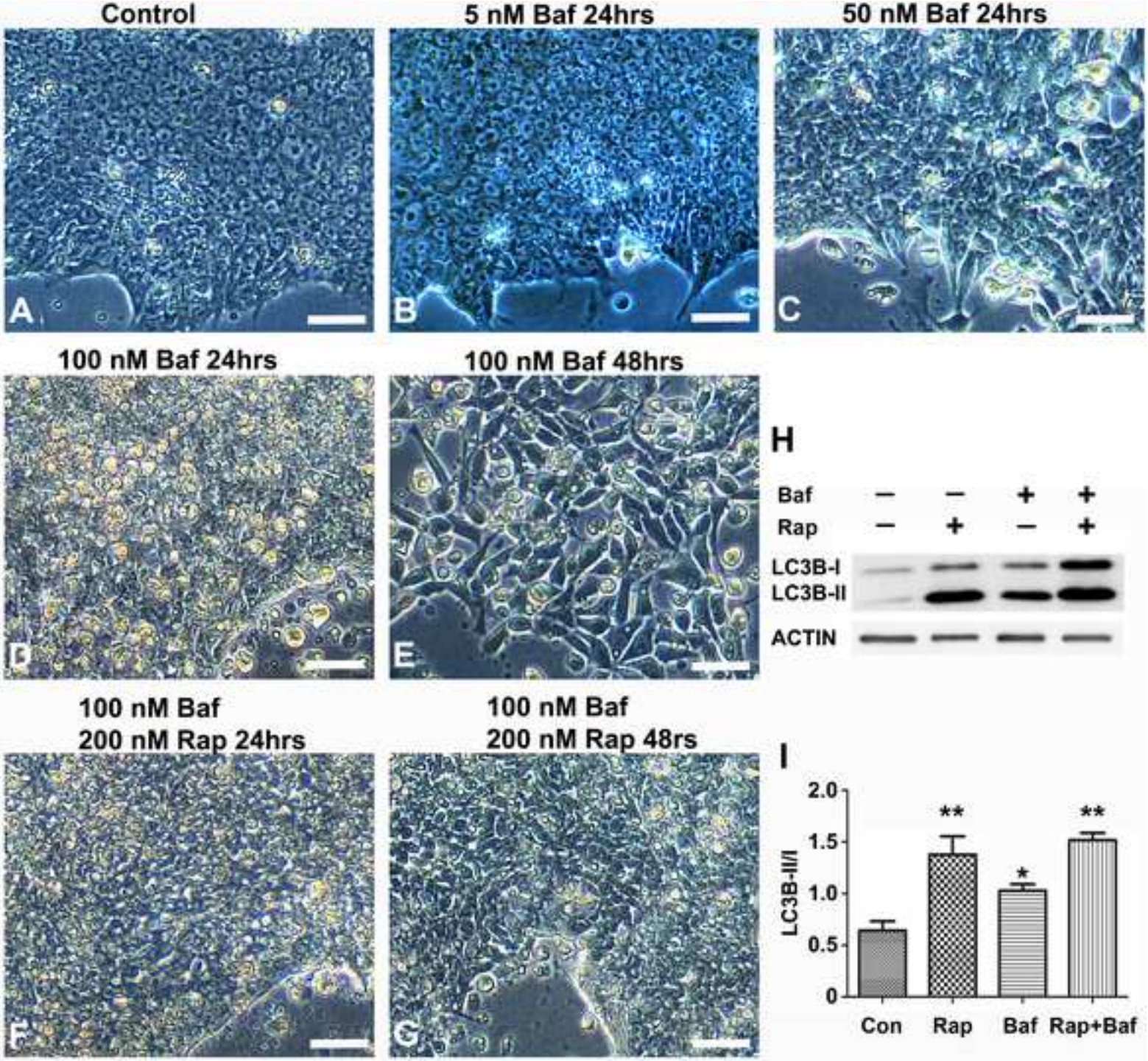

Figure 6

Click here to download Figure ShenFig 5 SCRT.tif

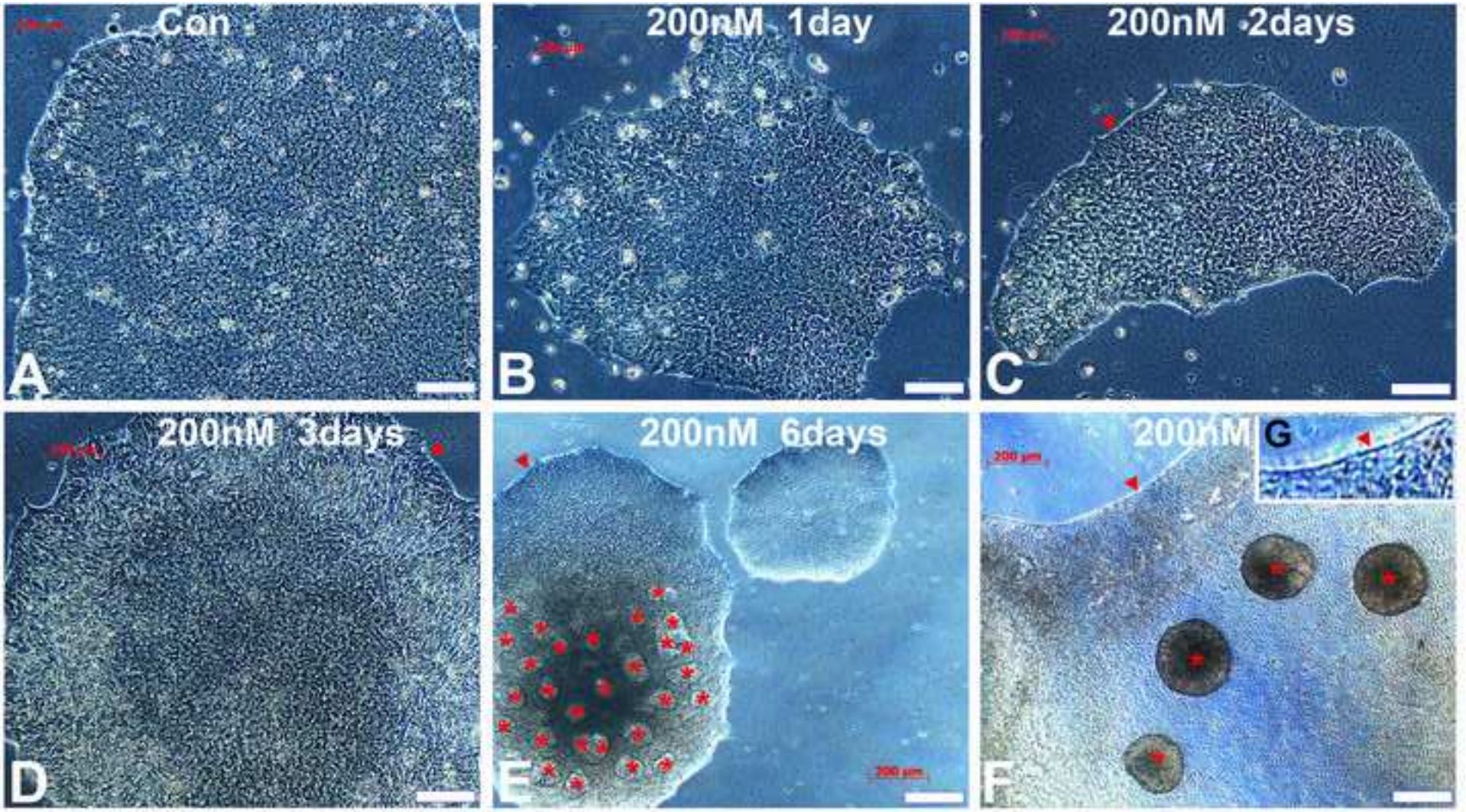

Figure 7

Click here to download Figure Fig 7 SCRT flat R1.tif

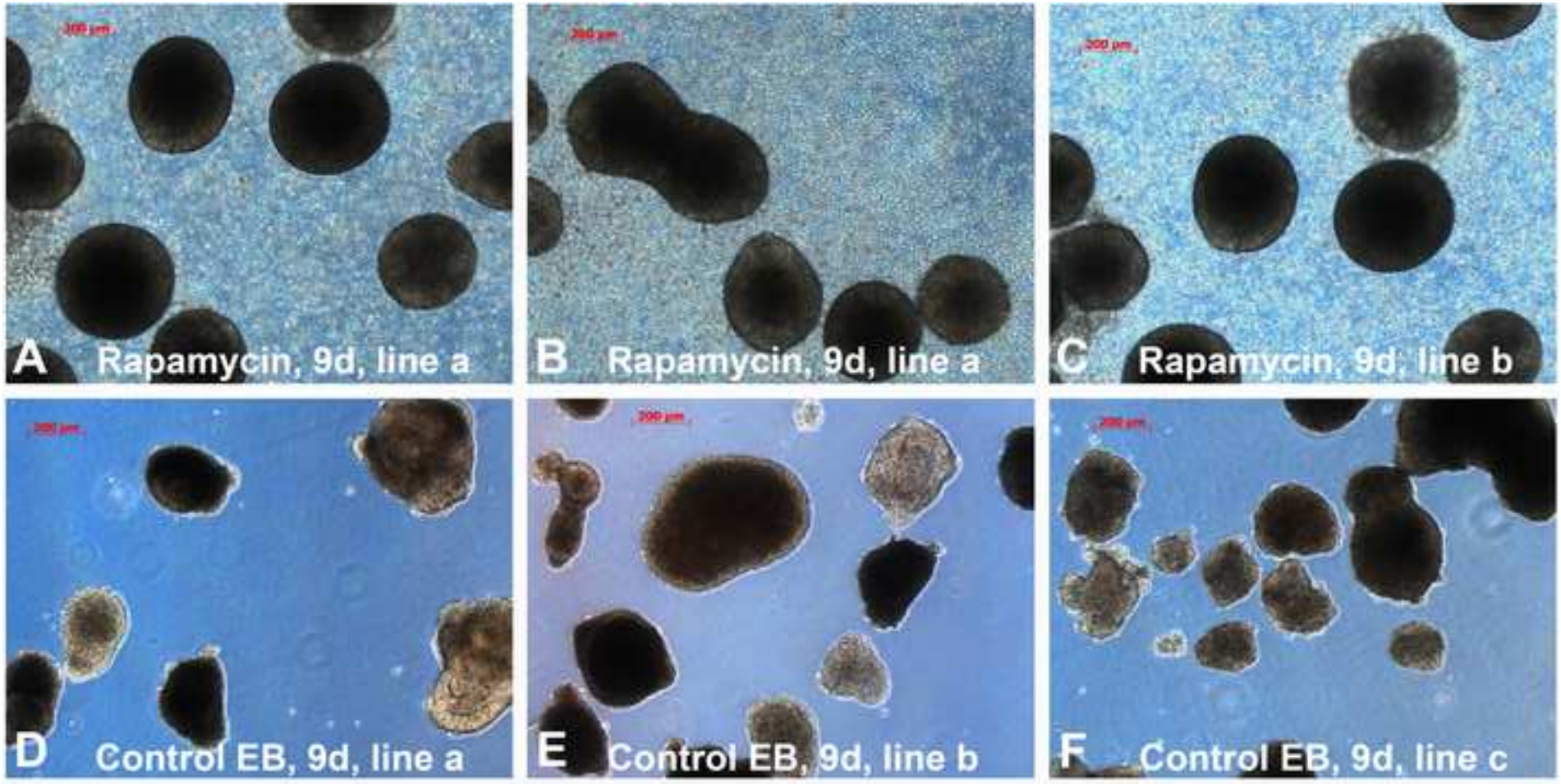

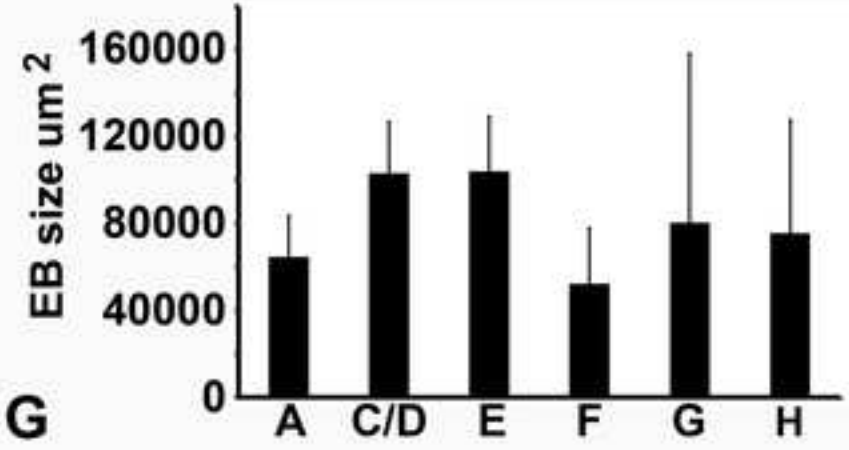

Figure 8

Click here to download Figure ShenFig 8 R1.tif

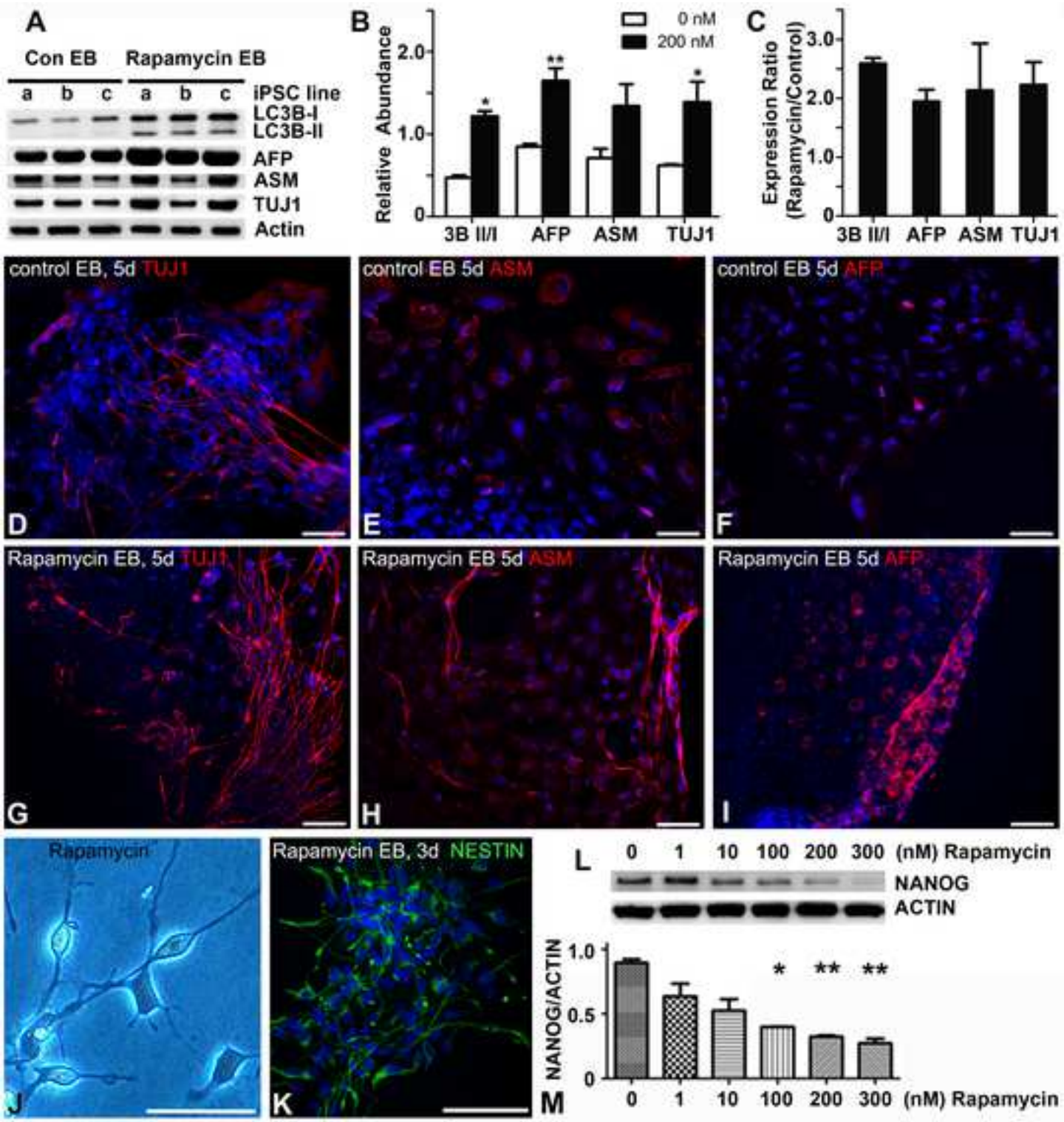

Figure 9

Click here to download Figure ShenFig 8 SCRT.tif

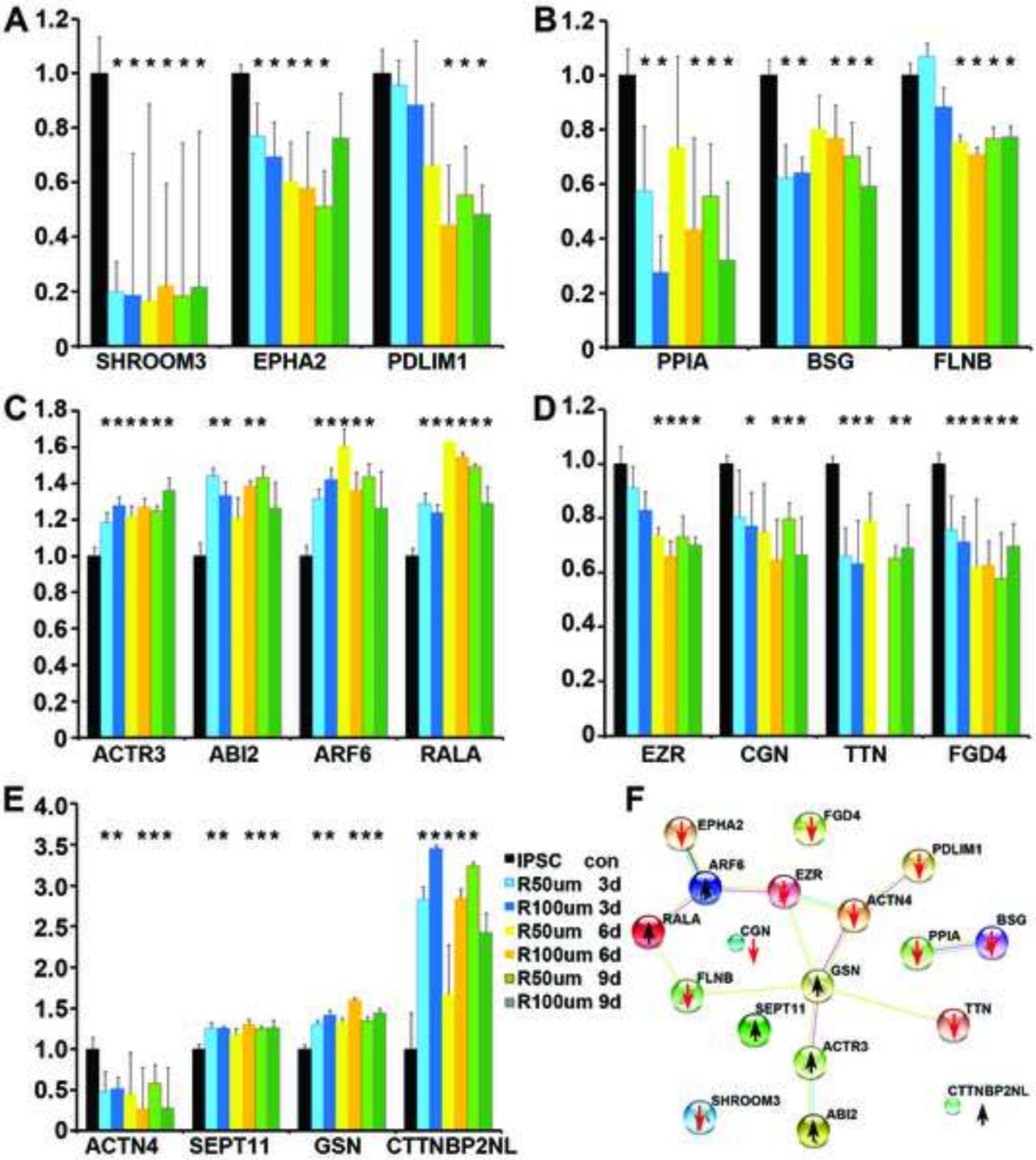

supplemental Figure 1

27 Sept., 2016

Submission of Revised Manuscript: **"Rapamycin Regulates Autophagy and Cell Adhesion in Induced Pluripotent Stem Cells"**

Dear Editor,

We thank you very much for your kind invitation. We have done additional experiments to carry out a comprehensive revision for the manuscript "**Rapamycin Regulates Autophagy and Cell Adhesion in Induced Pluripotent Stem Cells"** by Sotthibundhu *et al*, with point-to-point response to address Reviewers' constructive comments. The texts are revised accordingly with key revision data including:

Figure 1: we have provided fibroblasts image in Figure 1F and double staining images in Figure 1C.D.G.H.

Figure 3: we have supplied comparison with fibroblasts in Figure 3H by immunoblotting.

Figure 5: we added new Bafilimycin treatment data Figure 5A-I.

Figure 7: we removed duplicated image in Figure 7.

Figure 8: we removed duplicated images and supplied new mechanistic data of NANOG expression in Figure 8L-M.

Supplemental Figure 1: Immunoblotting of fibroblasts for LC3B expression.

We hope the revised manuscript has addressed major concerns and comments in the previous review process. We will be delighted to hear if the manuscript has now reached the standard of SCRT for publication.

Kind regards

Sanbing Shen, PhD
Professor of Fundamental Stem Cell Biology,
Regenerative Medicine Institute,
School of Medicine, National
University of Ireland Galway (NUI) Ireland.
Tel: 00-353-91-494261 (office).
Email: sanbing.shen@nuigalway.ie.